Tensions in tillage: Reduction in tillage intensity associates with lower wheat growth and nutritional grain quality despite enhanced soil biological indicators

Matthias Waibel [a], Jennifer Michel [b], Maurine Antoine [b], Iñaki Balanzategui-Guijarro [c], Da Cao [d], Pierre Delaplace [b], Jacques Le Gouis [e], David Alvarez [e], Claire Léon [e], Sandy Manfroy [b], Jordi Moya-Laraño [c], Sibille Perrochon [e], Sara Sanchez-Moreno [f], Inés Santin-Montanya [f], José Luis Tenorio [f], Cécile Thonar [b,g], Hervé Vanderschuren [b,h], Dominique Van Der Straeten [d], Thomas Verlinde [b,h], Markus Weinmann [i], Sarah Symanczik [a,*]

[a] Department of Soil Sciences, Research Institute of Organic Agriculture (FiBL), Frick 5070, Switzerland
[b] Plant Sciences, Plant Genetics and Rhizosphere Processes laboratory, Gembloux Agro-Bio Tech, TERRA teaching and research centre, University of Liège, Gembloux, Belgium
[c] Functional and Evolutionary Ecology, EEZA – CSIC, Almería, Spain
[d] Laboratory of Functional Plant Biology, Department of Biology, Faculty of Sciences, Ghent University, Ghent, Belgium
[e] INRAE, Génétique, Diversité et Ecophysiologie des Céréales, Université Clermont-Auvergne, Clermont-Ferrand, France
[f] Department of the Environment and Agronomy, National Centre Institute for Agricultural and Food Research and Technology, INIA-CSIC, Madrid, Spain
[g] Agroecology Lab, Faculty of Sciences, Université Libre de Bruxelles (ULB), Brussels, Belgium
[h] Tropical Crop Improvement Lab, Department of Biosystems, Heverlee, KU Leuven, Belgium
[i] Institute of Crop Science, Nutritional Crop Physiology (340h), University of Hohenheim, Stuttgart 70593, Germany

ARTICLE INFO

ABSTRACT

Dryland ecosystems are particularly susceptible to the adverse effects of intensive agriculture, with intensive tillage exerting a major impact on soil health and its biotic components. The implementation of less disturbing soil management practices can be essential for preserving the soil environment and maintaining the diverse communities of microorganisms, micro- and mesofauna, which are vital contributors to soil fertility. In this study, we assessed soil chemical properties, soil biodiversity and functionality, and wheat crop growth across a tillage gradient encompassing no-tillage (NT), minimum tillage (MT), and standard tillage (ST). Results showed that reducing tillage intensity increased soil macronutrient levels and the abundance of soil biota. Overall, higher levels of bacterial and fungal marker genes and higher abundance of predatory acari were observed in MT and NT compared to ST. Also, nematode abundance increased by 25 % in MT and 50 % in NT, compared to ST. Similarly, community structure analysis revealed that tillage strongly influenced bacterial, fungal and acari community composition, reflecting a gradient of soil disturbance intensity. Corresponding to the increased abundance of soil biota, reducing tillage intensity increased microbial activity and soil functionality along the disturbance gradient. In addition, evidence of the formation of biocrust as a possible source of carbon input was found. Despite enhanced soil biological indicators in less intensive tillage systems, wheat growth, nitrogen uptake and grain B vitamin contents were higher in ST compared to NT. In addition, we observed a shift in technological grain properties across tillage practices. The higher root:shoot ratio (an indicator of nitrogen deficiency) and median root diameter (hormone-driven lateral expansion) in NT suggest that soil compaction could be a potential cause of reduced wheat performance. These results suggest that despite improved soil biological indicators, other factors such as low rates of N mineralization potential due to drought conditions during the study year and the prevalence of soil compaction may limit wheat performance in NT systems.

* Corresponding author.
E-mail address: sarah.symanczik@fibl.org (S. Symanczik).

1. Introduction

Dryland agro-ecosystems are particularly vulnerable to the detrimental effects of intensive tillage, which causes upturn and disruption of soil structure, reduction of soil organic matter (SOM) content, and ultimately altering soil biodiversity and functioning (Haddaway et al., 2017; Kraut-Cohen et al., 2020; Li et al., 2019). As studies have shown, reducing tillage intensity has the potential to increase topsoil SOM, reduce soil erosion, enhance water retention, and thus it can help to preserve the integrity of soils (Haddaway et al., 2017).

Soil organisms provide multiple agroecosystem services including nutrient cycling, mitigation of biotic and abiotic stresses and thus soil and plant health (Bender et al., 2023; Delgado-Baquerizo et al., 2016, Delgado-Baquerizo et al., 2020; Wagg et al., 2019, Wagg et al., 2021). Several studies have documented the beneficial impacts of reduced tillage on increasing the abundance of soil microorganisms (Chen et al., 2020; Essel et al., 2019; Helgason et al., 2009; Mathew et al., 2012; Morugán-Coronado et al., 2022) and micro- and mesofauna (Brévault et al., 2007, Postma-Blaauw et al., 2010, Betancur-Corredor et al., 2022).

Through the disruption of fungal mycelia, intensive tillage is suspected to negatively impact fungal communities (Roger-Estrade et al., 2010), while higher soil organic carbon (SOC) in less intensive tillage systems should enhance microbial abundance and activity (Lori et al., 2017; Ramírez et al., 2020). However, a recent meta-analysis found that the response of soil microbial diversity to tillage is highly variable and strongly depends on pedoclimate and plant growth stage (Li et al., 2024, de Graaff et al., 2019): While minimum tillage increased bacterial diversity by 7 %, there was no significant effect on fungal diversity compared to ploughed systems. Similarly, van Capelle et al. (2012) have shown that the effect of tillage intensity on the abundance of soil biota might differ depending on soil texture. Given the central role of local pedoclimatic conditions in modulating the impact of tillage practices on soil microbial communities, it is essential to approach each environmental context individually to gain a full understanding of their responses. This involves to further identify key organisms responsible in shaping the soil environment, including those within the soil micro- and mesofauna, which are often neglected.

So far, most field studies investigating belowground effects of tillage practices have focussed either on the abundance and/or community structure of soil biota or on soil functional properties but without a link to aboveground performance (van Capelle et al., 2012; Roger-Estrade et al., 2010). Furthermore, there is still limited understanding about the driving factors behind crop performance under different tillage practices, as literature presents contradictory results: the effects of no-tillage and minimum tillage reported in meta-analyses are ranging from negative to neutral effects (Young et al., 2021). The meta-analysis of Pittelkow et al. (2015) demonstrated best performance of no-tillage under rainfed conditions in dry climates, matching conventional tillage yields, while average yield of 50 crops reduced by 5.1 %. Thus, further studies are needed that link soil biodiversity and functioning with crop growth and grain quality.

In the present study we investigated how tillage intensity in a long-term field experiment affects soil properties and the interplay between soil biodiversity, functionality and crop performance. Winter wheat was grown in crop rotation comparing no-tillage (NT), minimum tillage (MT) and standard inversion tillage (ST). We assessed soil chemical, biological and functional properties to identify tillage practices enhancing belowground functioning. Soil chemical factors comprised a range of soil macro and micronutrients and soil pH. Soil biological variables included the abundance, diversity and community structure of soil micro- and macrobiota including bacteria, fungi, nematodes and acari. Soil functional properties focused on the C-, N- and P-cycling potential of the soil, substrate utilization potential and microbial activity in general. Further, in an effort to establish connections to various agronomic quality indicators of winter wheat, we characterised shoot and root traits, grain nutrients and B vitamins as indicators for nutritional quality as well as starch size distribution and gliadin and glutenin contents in grains as technological quality indicators.

We hypothesised that: i) tillage intensity would be negatively correlated to SOC, soil biodiversity and functionality, ii) tillage intensity would drive shifts in the community structure of soil biota, namely bacteria, fungi, nematodes and acari, and iii) that an increase in SOC and higher nutrient cycling potential could translate into an enhanced uptake of nutrients leading to higher wheat biomass and grain nutrient and B vitamin content.

2. Material and methods

2.1. Site and soil characteristics

The experimental field for this investigation was the "La Canaleja" long-term tillage comparison trial of the Spanish National Research Institute for Food Research and Technology (INIA-CSIC), established in 1994 outside Alcalá de Henares (Madrid, Spain, 40°30'55.0" N 3°18'37.1" W; 600 m a.s.l.). The soil texture is classed as a Loam (USDA classification) and the soil type as a calcic Haploxeralf. The climate is semi-arid Mediterranean with the majority of the average annual precipitation of 367 mm yr^{-1} [1994–2022] having occurred in the autumn, winter, and spring months. In recent years, the average monthly temperature in summer has increased by ca. 1.3 °C and rainfall amounts have decreased in the months October to May by average total of 67 mm (period 2017–2022 vs. 1994–2022, own climatic data recorded on-site). The fallow period in the year before and the full winter wheat growing season 2021–2022 in the vegetative period (October to sample taking at flowering stage in May) did not exhibit a large total precipitation deficit (+99 mm and −13 mm, for the periods respectively) as compared to the averages of the previous years (2017–2022). However, some months in the period January to May of 2022 were much drier as compared against the average 2017–2022 (total 14 mm vs. 39 mm). Especially, the months April, May, and June in 2022 exhibited a total precipitation deficit of 149 mm with increased temperatures as compared to 2021 (Table A1) that may have led to insufficient soil water supply and increased evapotranspiration with potential drought conditions and seen in decreased wheat yield levels (Table A1). Indeed, the soil moisture determined at sampling in May was extremely low at ca. 2.7 %, where another study by Santin-Montanya et al. (2020) reported around 10 % at wheat flowering stage for the years 2014–2016.

2.2. Experimental design

The three field tillage treatments consist of standard/conventional tillage (ST), minimum tillage (MT), and no tillage (NT) and are arranged in a randomized complete block design (4 blocks = treatment replicates) with 5 split-plots within each block of which four contain crop rotations (Fallow, winter wheat, vetch, barley) and the fifth containing a wheat monoculture. In the crop rotation before winter wheat, one year of bare fallow is employed to accumulate rainwater for subsequent wheat cropping. The tillage practices for ST consist of mouldboard ploughing (30 cm), chisel (non-inversion) ploughing (20/15 cm) for MT, and no tillage for NT with herbicide treatments when needed for weed control middle of May and always at the beginning of October before sowing. Further details on seeding, nutrient, pest, weed, and residue management, as well as crop performance, soil physico-chemical, and climate aspects on this long-term trial were reported in preceding studies (Gandía et al., 2021; Santin-Montanya et al., 2020; Santin-Montanya et al., 2017; Santin-Montanya et al., 2016; Santin-Montanya et al., 2013; Tellez-Rio et al., 2017; Guardia et al., 2016; Martín-Lammerding et al., 2011, 2015; Martin-Rueda, et al., 2007).

2.3. Field sampling and sample processing

Shoots, roots and soil from the split-plots of winter wheat (*Triticum aestivum* var. Marius) in crop rotation were sampled at flowering at the end of May 2022. Rhizosphere soil for the analysis of soil microbial communities (bacteria, fungi), microfauna (nematodes), and mesofauna (acari) was sampled as composite sample of five samples per plot. First, plants were cut at the crown and then a shovel was used to extract the root system and adjacent soil from an area diameter of 15 cm at two depths 0–10 cm and 10–20 cm. Nematodes were sampled from a combined depth of 0–20 cm only. The soil at the center of the extracted root system was shaken off and transferred to plastic bags for subsequent DNA and soil functional analyses. For mesofauna, samples were carefully taken at the edges of the sampling holes as intact pieces of soil blocks with a total volume of 250 mL per plot and kept in sturdy plastic containers to avoid structural disturbance. For nematodes, a combined sample of 200 g soil per plot was taken and kept in sealed plastic bags. In between wheat rows, 10–20 additional soil samples were taken from 0 to 20 cm depth and combined to obtain 2 kg per plot for soil chemical analyses. For analysis of root system architecture, two additional samples were taken per plot: One root sample was taken with a precise volume (h=20 cm, d=9 cm) using a pneumatic soil corer (Royal Eijkelkamp B.V, The Netherlands) to determine root length and other quantitative parameters of root system architecture within that soil cylinder and an additional sample was taken from the top 10 cm extracting the root crown to count first to third order lateral roots and measure the respective root angles. For each root sample, corresponding aboveground plant biomass was sampled and kept in paper bags for drying at room temperature. All soil and root samples were immediately cooled to 4 °C and transported to the lab. For further analysis, soil samples were sieved at 2 mm and stored at 4 °C for MicroResp® analyses or frozen at −20 °C for DNA and enzymatic anaylses.

Root samples were carefully washed with water over 1 mm sieves to separate roots from soil. Clean roots were subsequently stored in 70 % ethanol. For quantitative root traits such as total root length and network area, the washed root samples were transferred to petri dishes and arranged without overlap of roots. Samples were scanned (Epson flatbed, 600 DPI, Seiko Epson Corporation, Japan) and images were subsequently processed in RhizoVision Explorer (Seethepalli et al., 2021). The root crown samples were digitized using Nikon D3400 (Nikon, Tokyo, Japan) and images were processed in RhizoVision Explorer (Seethepalli et al., 2021) and phenotyped for root angles and lateral root growth (Trachsel et al., 2011). Afterwards, root samples were dried at 40 °C in paper envelopes and root dry mass was determined. Corresponding aboveground biomass was separated into leaves, shoots and heads and dry weight determined.

2.4. Soil chemical analysis

Soil gravimetric moisture content was determined by drying over night at 105 °C. Soil C and N (%) were determined on a Vario Max Cube (Elementar Analysensysteme GmbH, Langenselbold, Germany). Further soil elements were determined on inductively coupled plasma optical emission spectroscopy (ICP-OES, Agilent 5110, Agilent Technologies Inc, USA) with extractants as detailed in the following. $CaCl_2$ extraction matrix was used for pH determination and estimation of plant available Mg. Calcium Acetate Lactate (CAL) extraction matrix was used for reflecting plant available K and P (VDLUFA, (2016), Scherer and Weichmann (1994). Calcium chloride/DTPA (CAT) extraction matrix was used for estimating plant available Cu, Fe, Mn, P, and Zn (VDLUFA, 2008). Nitric acid and hydrochloric acid (Aqua regia (AR)/ King`s water) digestion was applied to determine total B, Ca, Cu, Fe, K, Mg, Mn, P, and Zn concentrations in soil (VDLUFA, 1991). B concentrations were below the detection limit of 10 mg kg^{-1}.

2.5. Soil micro- and mesofauna analyses

Acari and Collembola were extracted from 500 mL of soil using Berlese-Tullgren funnels with LED lamps (non incandescent 7 W bulbs of 600 lumens) for 15 days at constant temperature (23 °C) and stored in 70 % ethanol. To identify the collected specimens to family level, dichotomous keys were used, e.g. Krantz and Walter (2009) for Acari and Jordana and Arbea (1989) for Collembola. The specimens were preserved in 70 % ethanol or mounted in semi-permanent slides with Hoyer's medium, and have been deposited in the "Mesofauna collection" at the Arid Zones Experimental Station (EEZA-CSIC). Only 4 specimens of Collembola were collected in total and we will therefore omit them from further discussion. To assign mite families to trophic guild (predator, fungivore, herbivore) the information in Krantz and Walter (2009), in addition to expert knowledge (e.g. shape of the mouth parts), were considered.

Nematodes were extracted by a modification of wet sieving and the Baermann funnel method (Barker, 1985). All nematodes were counted under a dissecting microscope and at least 100 individuals were identified to genus level under a light microscope after Bongers (1990). Nematode abundances were expressed as number of individuals 100 g fresh soil^{-1}. Nematode genera were classified into five trophic groups (bacterivores, fungivores, herbivores, omnivores, and predators) after Yeates (1994), and into the colonizer-persister (cp) scale, that classifies nematodes into five cp groups (cp1–5). Nematodes in low cp groups (cp 1–2) are commonly r-strategist bacterivores and fungivores with high reproduction rates, short life cycles, and resistance to environmental perturbation, while high cp groups (cp 3–5) are K-strategists with progressively longer life cycles, lower reproduction rates and higher sensitivity to perturbation and environmental stress (Bongers, 1990). Based on such functional classifications, nematode participation on nutrient cycling was assessed through the use of three nematode-based indices (Ferris, et al., 2001; Ferris, 2010). The Enrichment Index (EI) is based on the relative abundances of bacterivores with low cp value which are enrichment-opportunists, and is used as an indicator of fast organic matter decomposition mediated by bacteria and active nutrient cycling. The Channel Index (CI) is based on the ratio fungivores to opportunistic bacterivores and is used as an indicator of slow organic matter decomposition mediated by fungi. Both the EI and the CI range from 0 (no enrichment opportunists (EI) or fungal feeders (CI) present in the community) to 100 (absolute dominance of such functional groups). Finally, the Enrichment Footprint (EF) is a calculation of the potential amount of C mineralized (µg C kg^{-1} soil) by enrichment opportunistic nematodes and thus an indicator of the magnitude of the participation of such nematodes in the nutrient mineralization soil service.

2.6. Molecular microbial analysis

2.6.1. DNA extraction

DNA was extracted from 350 mg fresh weight soil using the Macherey Nagel NucleoSpin 96 Genomic DNA soil kit with the enhancer solution following the manufacturers recommendations. Prior to extraction, samples were homogenized twice for 5 min in a TissueLyser (Qiagen, Hilden, Germany) at 30 Hz in two different orientations and stored at −20 °C. Extract quality was checked with Nanodrop 260/230 and 260/280 nm absorption and on 1.5 % agarose gel electrophoresis. DNA concentration was quantified with Qubit dsDNA HS Assay Kit on 384 well plate reader (Tecan 200 Pro M Nano+).

2.6.2. Quantitative PCR

DNA extracts were diluted 10-times for quantitative PCR in a CFX384 Real-Time System (Bio-Rad Laboratories, CA, USA). Prokaryotic 16S marker gene quantification was performed in triplicate PCR reactions of 15 µL consisted of 7.5 µL 1x KAPA SYBR Fast qPCR Kit Master Mix 2 × Universal (Axonlab, Baden, Switzerland), 1.8 µL of each 10 µM forward and reverse primer (BactQuant, Liu et al., 2012) and 2 µL of DNA

template. Reaction conditions consisted of an initial denaturation at 95 °C for 3 min, and 39 cycles of denaturation at 95 °C for 15 s, annealing at 62 °C at 15 s, with final extension at 72 °C for 30 s. Melt curve analysis was performed from 65 to 98 °C. The amplification efficiency was between 68.9 % and 70.6 % and R^2 99.7–99.8 %. Prokaryotic copies were quantified against a ten-fold dilution series in triplicate of a 465 bp long target region on pJET 2974 plasmid (CloneJET PCR Cloning Kit, Thermo Fisher Scientific, Switzerland). Eukaryotic/fungal 18S marker gene quantification was performed in triplicate PCR reactions of 15 μL consisted of 7.5 μL 1x KAPA SYBR Fast qPCR Kit Master Mix 2 × Universal (Axonlab, Baden, Switzerland), 0.75 μL of each 10 μM forward and reverse primer (FR1 and FF390, VAINIO and HANTULA, 2000) and 2 μL of DNA template. Reaction conditions differed to the bacterial qPCR in that 35 cycles were carried out with annealing at 50 °C. The amplification efficiency was between 92.8 % and 95.9 % and R^2 99.6–99.9 %. Eukaryotic copies were quantified against a ten-fold dilution series in triplicate of a 390 bp long target region on pJET 2974 plasmid (CloneJET PCR Cloning Kit, Thermo Fisher Scientific, Switzerland).

2.6.3. Metabarcode analysis of bacterial and fungal community

Bacterial and fungal amplicon libraries were performed in a limited cycle PCR amplification approach followed by an Illumina barcode indexing PCR for sample pooling (Symanczik et al., 2025). For amplification of the 16S V3-V4 target region, primers 341 F (5´-CCTAYGGGDBGCWSCAG-3') and 806 R (5'-GGACTACNVGGGTHTC-TAAT-3') (Frey et al., 2016) were used with added nextera and sequencing adaptors. The fungal ITS2 target region enclosed by the 5.8S and 28S gene cassette was amplified with ITS3ngs (5'-CANCGATGAA-GAACGYRG-3') and ITS4ngs (5'- CCTSCSCTTANTDATATGC-3') (Tedersoo and Lindahl, 2016) and the same adaptors as used for bacteria. The first PCR was performed in triplicate PCR reactions of 15 μL consistent of 7.5 μL 1x KAPA SYBR Fast qPCR Kit Master Mix 2 × Universal (Axonlab, Baden, Switzerland), 0.4 μL each of 10 μM forward and reverse primers, and 2 μL of DNA template of different DNA template dilutions (1:5, 1:10, 1:25 for bacteria and 2 x original concentration and 1:5). The reaction conditions for bacterial and fungal sets consisted of initial denaturation at 95 °C for 3 min, followed by 35 cycles (bacteria) or 40 cycles (fungi) of denaturing 95 °C for 20 s, annealing 58 °C (bacteria) and 60 °C (fungi) for 15 s and extension 72 °C for 40 s and a final extension at 72 °C for 10 min. Triplicate reactions were pooled and purified using a magnetic bead solution (https://openwetware.org/wiki/SPRI_bead_mix) and visualized on agarose gel (1.5 %). The indexing PCR step was carried out as per default instructions of the Ilumina indexing kit where the template concentration was prediluted to 0.1–0.5 ng DNA μL-1. Index PCR reactions were purified using a magnetic bead solution (https://openwetware.org/wiki/SPRI_bead_mix), visualized on agarose gel (1.5 %) and quantified with Qubit dsDNA HS Assay Kit on a 384 well plate reader (Tecan 200 Pro M Nano+) before library pooling. Final libraries were quantified and size checked with TapeStation (4150 TapeStation System, Agilent Technologies, Switzerland). Both libraries including non-template PCR/library control (n = 1) and processing blanks (n = 2) were sequenced separately on Illumina MiSeq v3 (Illumina Inc., San Diego, CA, USA) paired end 2 × 300 bp sequencing at Genome Quebec CES (Montreal, Canada) with ~7 % PhiX per sequencing run. Libraries were deposited to NCBI SRA and are available under accessions PRJNA1198325 and PRJNA1198337.

Sequencing reads were prepared at Genetic Diversity Center (GDC), ETH Zürich, in the USEARCH pipeline. Reads were demultiplexed, PhiX and low complexity samples were removed, and reads trimmed at each end with 30 or 55 bp length. Read pairs were synchronized, merged with minimum 30 bp overlap, 100 bp length, and 60 % identity, and primer sites removed in-silico. Size and quality of amplicons was selected at 300–500 bp length for 16S and between 200 and 500 bp for ITS2 with minimum mean Q score of 20 leaving 6.4 mil. (5.5 mil. unique) and

11.2 mil. (1.7 mil. unique) amplicons for 16S and ITS2 sets, respectively. UNOISE3 was used to deduplicate amplicons and denoise sequences with zero radius operational taxonomic units clustered de-novo at 97 % similarity (97 % zOTUs). Amplicons were backmapped to OTUs (counting). Taxonomy assignment was made with SINTAX for 16S against SILVA SSU v138 (RESCRIPt) (Quast et al., 2012) with tax filter at 0.75. For ITS2, taxonomy assignment was made against UNITE Eukaryotes USEARCH/UTAX release v83 (Nilsson et al., 2019) with tax filter at 0.75. Additionally, ITSx (Johan Bengtsson-Palme et al., University of Gothenburg Version: 1.1.3) was used to extract and identify the ITS region. Reads that were not classified as fungi based on ITSx were removed prior to further cleaning detailed in the next section. Cleaning of non-target taxa and contaminants was done on the whole set before splitting into the field experiments. For the 16S data, archaea, mitochondria and chloroplasts were removed. All taxa (n = 13) found in NTC and blanks were removed from analysis. The average bacterial read count was 18,355 reads, minimum reads at 7793, consisting of 1666 taxa, and with a data sparsity of 35 %. For the ITS2 dataset, all phyla other than fungi and taxa found in NTC and blanks (n = 214) were removed. On average 14,012 reads remained with a minimum at 7042 reads of 1,277 taxa with a data sparsity of 75 %.

2.7. Soil functionality

Activities of seven hydrolytic extracellular enzymes were measured, including four enzymes involved in C-acquisition: α-glucosidase, β-glucosidase, cellobiohydrolase, β-xylanase; two enzymes involved in N-acquisition: leucine aminopeptidase, β-N-acetylglucosaminidase, and one enzyme involved in P-acquisition: phosphatase. Extracellular enzyme activity (EEA) was assessed using standard fluorometric techniques and the activities, represented by nmol g^{-1} dry soil h^{-1}, of the C, N, and P acquiring enzymes were grouped to represent the general potential C, N, and P acquisition activity in soil samples (Bell et al., 2013).

Chemotrophic, respiratory soil CO_2 evolution upon addition of different substrates was determined with Microresp™ system (Campbell et al., 2003). Absolute respiration rates (μg CO_2–C g^{-1} dry soil eq. h^{-1}) were calculated as shown in the MicroResp™ technical manual (Cameron, 2007). For each sample, eight technical replicates were measured and obvious outliers removed (coefficient of variance > 20). In addition, reference soils were included as standards in each run (Creamer et al., 2016). Soils were pre-incubated for one week at the later assay temperature and soil basal respiration was measured as soil samples supplemented with deionized water, and multiple substrate-induced respiration (MSIR) as the total CO_2 flux from all substrates (keto-glutaric acid, oxalic acid, xylan, glucose, N-acetyl-glucoseamine, alanine, amino-butyric acid). Microbial biomass (SIR-MBC) was estimated from the glucose (ca. 59 mg g^{-1} soil dry weight eq.) induced average respiration rate volume after 5 h of incubation and using the formula from Anderson and Domsch (1978). The metabolic quotient (qCO2) was calculated as basal respiration over SIR-MBC (Wardle and Ghani, 1995; Anderson and Domsch, 2010).

2.8. Wheat harvest analysis

At maturity, grains were harvested using a plot harvester. Grain yield was assessed after cleaning and air drying the grains. Thousand-kernel weight was measured with an Opto-Agri (Optomachine, Riom, France). For mineral nutrient analyses in wheat grains, dried and milled samples were mineralized by microwave (UltraClave V Fa. MLS Leutkirch, Germany) digestion with HNO_3. (VDLUFA, 2021). In samples where silicon was to be analyzed, a second microwave digestion was performed and subsequently 0.5 mL HF were added to inhibit polymerization and precipitation of the dissolved silica. Grain nutrient analysis of C, N, S was determined via Elemental-Analyzer (Elementar Vario EL, Elementar Analysensysteme GmbH, Langenselbold, Germany; VDLUFA, 2012), Cl on Ion Chromatography (Integrion, Thermo Fisher

Scientific, Waltham, MA, USA; VDLUFA, 2019), Ca, Cu, Fe, K, Mg, Mn, Na, P and Si on inductively coupled plasma optical emission spectroscopy (ICP-OES, Agilent 5110, Agilent Technologies Inc, USA), Co, Mo, Ni, and Se on ICP-MS (Perkin Elmer NexION 300 X, PerkinElmer, Waltham, MA, USA), and I with ammoniacal extraction on ICP-MS (Perkin Elmer NexION 300 X, PerkinElmer, Waltham, MA, USA). All analyses were conducted at Core Facility University of Hohenheim, Analytical Chemistry Unit. All Na and I was below the detection limit at 20 mg kg^{-1} or 0.5 mg kg^{-1}, respectively. Most values of Se were below detection limit at 0.025 mg kg^{-1}. For Si and Co some values were below detection limit and were replaced with half detection limit value at 150 mg kg^{-1} and 0.025 mg kg^{-1}, respectively.

Analysis of seven grain B vitamins was performed as reported previously (Cao et al., 2024). Briefly, around 50 mg of homogenized wheat seeds were extracted with 1 mL of 50 mM phosphate buffer containing internal standards for each type of B vitamin. The extract was treated with multi-enzyme incubation to release protein-bound forms and associated bioactive derivatives and analyzed with liquid chromatography coupled with tandem mass spectrometry (UHPLC-MS/MS).

Technological properties of wheat grains included the distribution of starch size classes distinguishing between A-type ($>10\,\mu m$), B-type ($2–10\,\mu m$) and C-type ($<2\,\mu m$) starch and grain glutenins and gliadins contents. The size distribution of the purified starch granules was estimated with a Mastersizer 2000E laser particle size analyzer and the Hydro 2000SM small volume wet sample dispersion unit (Malvern Panalytical Ltd, Palaiseau, France) following the protocol reported by Edwards et al. (2008). Protein composition was determined after sequential extraction. Briefly, 66.6 mg fresh weight of complete flour were mixed with 1 mL of 50 mM phosphate buffer (pH 7.8) containing 100 mM NaCl (30 min, 800 rpm, 4 °C). After centrifugation (10 min, 18, 000 g, 4 °C), the pellet was mixed with 1 mL of the same 50 mM phosphate buffer (10 min, 800 rpm, 4 °C) and centrifuged in the same condition. This operation was repeated once. To extract gliadins the pellet was mixed with 1 mL 70 % ethanol (30 min, 1100 rpm, 4 °C). After centrifugation (10 min, 18,000 g, 4 °C), extraction was done with the same 70 % ethanol buffer (10 min, 1100 rpm, 4 °C) and centrifuged. This operation was repeated twice. After each centrifugation the supernatant containing gliadins was collected and pooled. Finally, to extract glutenins the resulting pellet was mixed with 0.5 mL of 25 mM borate buffer (pH 9.8) containing 50 % propanol-2 and 1 % DTT (30 min, 1200 rpm, 50 °C) and centrifuged (10 min, 18,000 g, 18 °C). This operation was repeated once. After each centrifugation the supernatant containing glutenins was collected and pooled. For stability, glutenin fraction was alkylated with 4.6 % of 4-Vinylpyrridine (15 min, 60 °C). The two glutenin subunits (High-Molecular Weight Glutenin Subunit, HMW-GS; Low-Molecular Weight Glutenin Subunit, LMW-GS) and four gliadin classes (α/β-, γ-, ω1,2-, ω5-gliadin) were quantified by reverse phase high performance liquid chromatography (RP-HPLC) using an Agilent 1290 Infinity LC system (Agilent Technologies, California, USA) as described by Dai et al. (2015). Briefly, gliadin and glutenin extracts were filtered through regenerated cellulose syringe filters (0.45-μm pore diameter, UptiDisc, Interchim, Montluçon, France), then 4 μl of each protein extract were injected into a C8 reversed-phase ZORBAX 300 Stable Bound column (2.1 × 100 mm, 3.5 μm, 300 Å; Agilent Technologies) maintained at 50 °C. Proteins were separated at a flow rate of 1 mL/min using linear solvent gradients from 24 % to 50 % acetonitrile containing 0.1 % (v/v) trifluoroacetic acid over 13 min for gliadins, and from 23 % to 42 % over 25 min for glutenins. Proteins were detected by UV absorbance at 214 nm. Chromatograms were processed with ChemStation 10.1 software (Agilent Technologies) and the HPLC peaks corresponding to each of the four gliadin classes and the two glutenin subunits were identified following the observations of Wieser et al. (1998). All quantities were corrected to consider the extraction yield which was estimated to be 93 % for all fractions. In addition, the glutenin quantities were then corrected to consider the extraction yield without SDS which was estimated to be 70 % (Nicolas et al., 1998).

Protein quantities were determined with a calibration curve based on the Dumas combustion method using a FlashSmart N Analyzer (ThermoScientific, Villebon-sur-Yvette, France).

2.9. Statistical analyses

For data handling, descriptive analysis, and plotting *R* version 4.3 (R Core Team, 2023) was used with tidyverse, grid and gridExtra packages (Wickham et al., 2019; R Core Team, 2023; Auguie, 2017). Hulls were drawn with ggConvexhull (Martin, 2017) and labels with ggRepel (Slowikowski, 2023).

Treatment effects on univariate data (soil chemical, wheat traits, organism abundance, Shannon diversity, and functional activity) were tested by ANOVA with linear model of block and management as fixed factors when from one/composite depth. The models for ratio of eukaryotic to prokaryotic qPCR values and root to shoot ratio were tested as ANCOVA with nominator as response and denominator as covariate. Values were Box-Cox transformed when multiple DHARMa diagnostics (Hartig, 2022) indicated violations. Models that still failed in DHARMa diagnostics are reported in brackets. Fixed factors were tested with type III ANOVA. With data from two depths, (Generalised) Linear Mixed effect Models (GLMM, GLM, or LMM) were used as appropriate for type of response variable with block, management, depth, and management:depth interaction as fixed factors and plot as random factor. The metabolic quotient as the ratio of basal respiration over biomass was modelled as LMM in glm function with denominator as B-spline in splines package (R Core Team, 2023). For acari count data, GLMM with negative binomial family was used after comparing Akaike`s information criterion with Poisson family model. For LMM models, fixed factors were tested with type III ANOVA, Kenward-Roger F-test and Satterthwaite's degrees of freedom. For GLM and GLMM models, fixed factors were tested with type II ANOVA and Likelihood Ratio test or Wald Chi square test, respectively. For all models, values reported are estimated marginal means from linear combination of model coefficients and were back-transformed for reporting. Brackets report the 95 % confidence interval (CI). R packages used were base stats, spline, lme4, glmmTMB, lmtest, DHARMa, emmeans, car & effects, and multcomp (R Core Team, 2023; Bates et al., 2015; Brooks et al., 2017; Zeileis and Hothorn, 2002; Hartig, 2022; Lenth, 2023; Fox and Weisberg, 2019; Hothorn et al., 2008).

For amplicon sequencing data, rarefaction was made to the minimum sequencing depth sample (Schloss, 2024) with vegan`s rrarefy (Oksanen et al., 2022). Rarefaction with 999 repeats was used for repeatedly calculating alpha and beta diversity indices for averaging over sub-sampling results. Beta diversity (site dissimilarity) for bacteria, fungi, acari and nematode data was calculated with Bray-Curtis index (Bray and Curtis, 1957). Alternatives such as e.g. centered-log ratio transforms and Aitchison`s distance to address compositionality (Gloor et al., 2017, Zhou et al., 2022), were also checked (not shown), but were argued to be unnecessary to control type I error of community-wide tests (Zhou et al., 2022). Homogeneity of multivariate group dispersions were tested with betadisper test (Anderson, 2006) in vegan at 5 % significance level. Clustering with unweighted pair-group method arithmetic average (UPGMA) and ordination of sample to sample dissimilarities were done with Principal Coordinate Analysis (PCoA) in base R cmdscale function, respectively. Significance of tillage and depth factors (incl. interactions) on community dissimilarity were determined with the permutational multivariate ANOVA (perMANOVA) (Anderson, 2006) in vegan with 9999 permutations and restricting permutations to block when block was found to be significant at p < 0.05.

Differential abundance of bacterial and fungal taxa was determined with LinDA (Zhou et al., 2022) at 5 % FDR on the rarefied dataset and using centered log-ratio transform (Yang and Chen, 2023, 2022). Combinations of depth and tillage, and block were considered as fixed factors and plot as random factor. Contrasts with significantly differential abundant taxa were retrieved from model coefficients in LinDA

Wald test with multiple test correction by the Benjamini-Hochberg method. In this dataset, especially for the sparse fungal set, the LinDA method reported conservative positive detections among other tools employed, such as for example DESeq2 (Love et al., 2014) or per taxon application of glmmTMB (Brooks et al., 2017) (not shown). For cluster analysis, significant taxa were gathered and their log2 transformed counts (+1 pseudo-count) subtracted from their global mean, Euclidean distances calculated, and hierarchically clustered with Ward's rule (Love et al., 2014). Heatmaps were drawn in pheatmap package (Kolde, 2019) and the number of informative "change" clusters were identified with Gap statistic (b=999 folds) and the Tibshirani et al. (2001) criterium in cluster package (Maechler et al., 2022, Akalin, 2020). The silhouette (similarity) value (Rousseeuw, 1987) of clusters and taxa to their peers was calculated (Akalin, 2020).

3. Results

3.1. Effects of tillage intensity on soil properties

Soil chemical and physical properties were analyzed to assess the effect of tillage intensity on soil properties after running for almost 30 years. Results showed that total C and N in both depths sampled (0–10 and 10–20 cm) were twice as large in NT as compared to ST and MT ($p < 0.05$, Table 1). Similarly, significantly highest concentrations of total soil P (P_{AR}) and plant available K (K_{CAL}) were found in NT ($p < 0.05$, Table 1). Concentrations of other macro- and micronutrients were similar across tillage treatments (Table 1), thus data for plant available Cu, Fe, Mn, P, and Zn measured using Calcium chloride/DTPA (CAT) extraction are not shown, but are available on Zenodo (https://doi.org/10.5281/zenodo.15007358). Soil moisture contents were low in all treatments ranging between 2.6 % and 3.2 % with significantly lowest values in NT compared to MT and ST ($p < 0.05$).

3.2. Impact of tillage intensity on soil biodiversity

To assess the impact of tillage intensity on soil biodiversity, a range of biological indicators based on molecular and classical morphological assessments were analyzed. Reducing tillage intensity (MT and NT) significantly increased the abundances of gene copy numbers of prokaryotes and eukaryotes as compared to ST ($p < 0.05$, Table 2). The ratio of eukaryotic to prokaryotic gene copies in topsoil increased on average

with reduction of tillage intensity from 0.12 in ST, over 0.13 in MT, to 0.15 in NT. Acari were found to be on average most abundant in NT. In particular, predatory acari were significantly most abundant under NT (Table 2). Of note was that total and fungivore acari were significantly more abundant in ST than in MT. Nematode abundance did not differ significantly across tillage treatments. On average, total abundance of nematodes, including their trophic groups such as bacterivores, fungivores, and herbivores increased consistently from ST over MT to NT (Table 2). This trend parallels the increase in prokaryotic and eukaryotic gene copies (Table 2). Regarding community richness and evenness of the respective communities, as assessed by the Shannon index, the bacterial diversity was found to be significantly reduced in NT ($p < 0.05$), while the diversity of other communities did not differ significantly with tillage intensities (Table 2).

Multi-taxa community composition dissimilarities as calculated using the Bray-Curtis index were ordinated by Principal Coordinate Analysis (PCoA) for bacteria, fungi, acari and nematodes. This showed in 2D space a gradient along with tillage intensity (Fig. 1 A–D). Permutational ANOVA supported this finding by indicating significant effects of tillage intensity ($p < 0.05$) on bacterial, fungal and mite communities, but not on nematodes (Table A2). Soil depth was not found to be a significant factor in community composition.

Taking a closer look at the structure of bacterial communities across all treatments, Planctomycetota constituted the relatively most abundant phylum at 39.0 % followed by Acidobacteria (15.8 %), Actinobacteriota (14.4 %), Proteobacteria (8.6 %), Chloroflexi (8.5 %), and Verrucomicrobiota (7.9 %) (Fig. A1). Besides Cyanobacteria, which showed the most pronounced tillage-induced shifts in relative abundance increasing from 0.5 % under ST and MT to 3.8 % under NT, several other taxa also changed (supplementary file A1).

Differential abundance analysis showed that 136 bacterial taxa were significantly associated with tillage and only one with depth (LinDA, FDR<5 %). These candidates represented the maximum of 23 % (NT, 0–10 cm) and minimum of 17 % (MT, 10–20 cm) of 16S rRNA gene counts. The change profiles of these bacteria clustered according to Gap statistic and Tibshirani criterion into seven informative groups (Fig. A2). Clusters 7, 6 and 3, in order of decreasing mean log-fold change, were characterized by relative increases of bacteria under NT. A taxon from the genus *Tychonema* (order Cyanobacteriales) in cluster 7 was particularly prominent in terms of high relative abundance at 3.5 % at 0–10 cm depth and 3.3 % at 10–20 cm depth under NT and its high

Table 1

Soil chemical properties standard tillage (ST), minimum tillage (MT) and no-tillage (NT) systems, in order of decreasing tillage intensity, collected from 0 to 10 cm, 0–20 cm, or individually from 0 to 10 cm and 10–20 cm as indicated. Extraction matrices used are abbreviated as follows: Calcium Chloride ($CaCl_2$), Calcium-Acetate-Lactate (CAL), nitric acid and hydrochloric acid (AR, aqua regia). Values presented are estimated marginal means with 95 % confidence intervals given in brackets. Model outputs are indicated with $p \leq 0.05$ * , 0.01 * * , 0.001 * * *. Statistical analyses that failed ANOVA assumptions are reported in brackets. Different letters indicate significant differences between groups (α=0.05).

Soil property	Depth	Tillage	ST	MT	NT
Moisture content (%)	0–20 cm	$F_{2,6} = 8.7$ *	3.2 [3.0, 3.5] a	3.1 [2.9, 3.4] a	2.6 [2.4, 2.9] b
Soil pH$_{CaCl2}$	0–20 cm	$F_{2,6}=0.3$	7.4 [7.0, 7.7]	7.3 [7.0, 7.6]	7.2 [6.9, 7.5]
Total C (%)	0–10 cm	($F_{2,8}=9.6$ * *)	0.77	0.80	1.32
Total C (%)	10–20 cm	$F_{2,8}=10.0$ * *	0.73 [0.65, 0.84] b	0.79 [0.70, 0.95] b	1.24 [0.94, 1.34] a
Total N (%)	0–10 cm	$F_{2,8}=29.1$ * * *	0.06 [0.05, 0.08] b	0.07 [0.06, 0.08] b	0.12 [0.11, 0.13] a
Total N (%)	10–20 cm	$F_{2,8}=16.2$ * *	0.06 [0.04, 0.07] b	0.07 [0.05, 0.08] b	0.11 [0.09, 0.12] a
C:N ratio	0–10 cm	($F_{2,8}=0.6$)	12.1	10.9	11.4
C:N ratio	10–20 cm	($F_{2,8}=0.2$)	12.2	11.3	11.7
P $_{CAL}$ (mg kg^{-1})	0–20 cm	$F_{2,6}=4.1$	692 [499,884]	677 [484,869]	958 [766,1151]
P $_{AR}$ (mg kg^{-1})	0–20 cm	$F_{2,6}=68.1$ * * *	324 [310,340] b	335 [319,352] b	451 [425,480] a
K $_{CAL}$ (mg kg^{-1})	0–20 cm	$F_{2,6}=42.9$ * * *	1592 [1255,1960] b	1497 [1168,1857] b	3477 [3008,3973] a
K $_{AR}$ (mg kg^{-1})	0–20 cm	($F_{2,4}=0.1$)	5290	4624	4963
Mg $_{CaCl2}$ (mg kg^{-1})	0–20 cm	$F_{2,6}=0.3$	1602 [966,2238]	1458 [822,2093]	1742 [1106,2378]
Mg $_{AR}$ (mg kg^{-1})	0–20 cm	$F_{2,6}=3.0$	5688 [5061,6315]	4848 [4221,5475]	5501 [4874,6128]
Ca $_{AR}$ (mg kg^{-1})	0–20 cm	($F_{2,6}=0.6$)	5896	4554	5822
Fe $_{AR}$ (mg kg^{-1})	0–20 cm	$F_{2,6}=2.1$	18446 [16812,20080]	16743 [15109,18377]	16792 [15158,18426]
Mn $_{AR}$ (mg kg^{-1})	0–20 cm	$F_{2,6}=0.3$	310 [268,352]	295 [253,338]	292 [249,334]
Cu $_{AR}$ (mg kg^{-1})	0–20 cm	$F_{2,6}=0.8$	13 [12,14]	12 [11,13]	12 [11,14]
Zn $_{AR}$ (mg kg^{-1})	0–20 cm	$F_{2,6}=0.5$	46 [41,51]	43 [37,48]	44 [39,50]

Table 2

Abundances and diversity of soil bacteria, fungi, acari, and nematodes under standard tillage (ST), minimum tillage (MT) and no-tillage (NT) collected from 0 to 10 cm, 0–20 cm, or individually from 0 to 10 cm and 10–20 cm as indicated. Values presented are estimated marginal means with 95 % confidence interval given in brackets. Model outputs are indicated with p ≤ 0.05 * , 0.01 * * , 0.001 * ** . Statistical analyses that failed ANOVA assumptions are reported in brackets. Different letters indicate significant differences between groups (α=0.05).

	Unit	Tillage (T)	Depth (D)	T:D	ST	MT	NT
Abundance							
Prokaryotic 16S	Copies g^{-1} soil	$F_{2,8}$= 7.7 *	0–10 cm		5837 [3309,9479] b	14434 [9450,21018] a	15418 [10184,22294] a
Eukaryotic 18S		($F_{2,8}$=4.7 *)	0–10 cm		657	1761	2064
Ratio Eu:Pr	-	($F_{2,7}$=0.2 *) cov ns	0–10 cm		0.12	0.13	0.15
Nematodes total	Counts 100 g^{-1} soil	$F_{2,8}$=1.5	0–20 cm		1546 [698,2394]	1930 [1081,2778]	2448 [1600,3296]
Bacterivores		$F_{2,8}$=1.0	0–20 cm		939 [315,1562]	1269 [645,1892]	1469 [846,2092]
Fungivores		($F_{2,8}$=0.1)	0–20 cm		468	526	454
Herbivores		$F_{2,8}$=3.6	0–20 cm		95 [54,201]	96 [54,202]	301 [128,1121]
Omnivores		na			-	-	-
Predators		na			8	21	32
Acari total	Counts 500 mL^{-1} soil	χ^2= 15.1 * **	χ^2= 0.0	χ^2= 1.2	86 [49,151] a	25 [14,46] b	123 [70,216] a
Fungivores		χ^2= 14.3 * **	χ^2= 0.0	χ^2= 1.5	83 [47,148] a	24 [13,43] b	106 [60,187] a
Predators		χ^2= 13.6 * **	χ^2= 0.3	χ^2= 0.1	2 [1,5] b	1 [0,3] b	14 [6,30] a
Herbivores		Only four observations			-	-	-
Shannon diversity							
Bacteria		$F_{2,13}$= 11.1 * *	$F_{1,9}$= 4.3	$F_{2,9}$= 0.9	5.97 [5.91, 6.04] a	5.98 [5.91, 6.04] a	5.80 [5.73, 5.86] b
Fungi		$F_{2,17}$= 1.5	$F_{1,9}$= 0.0	$F_{2,9}$= 1.8	3.94 [3.47, 4.42]	4.49 [4.02, 4.96]	4.10 [3.63, 4.58]
Nematodes		$F_{2,8}$= 1.0	0–20 cm		1.41 [1.22, 1.68]	1.39 [1.21, 1.65]	1.59 [1.35, 1.68]
Acari		$F_{2,16}$= 0.2	$F_{1,9}$= 0.0	$F_{2,9}$= 2.1	1.34 [1.01, 1.67]	1.38 [1.04, 1.71]	1.78 [1.44, 2.11]
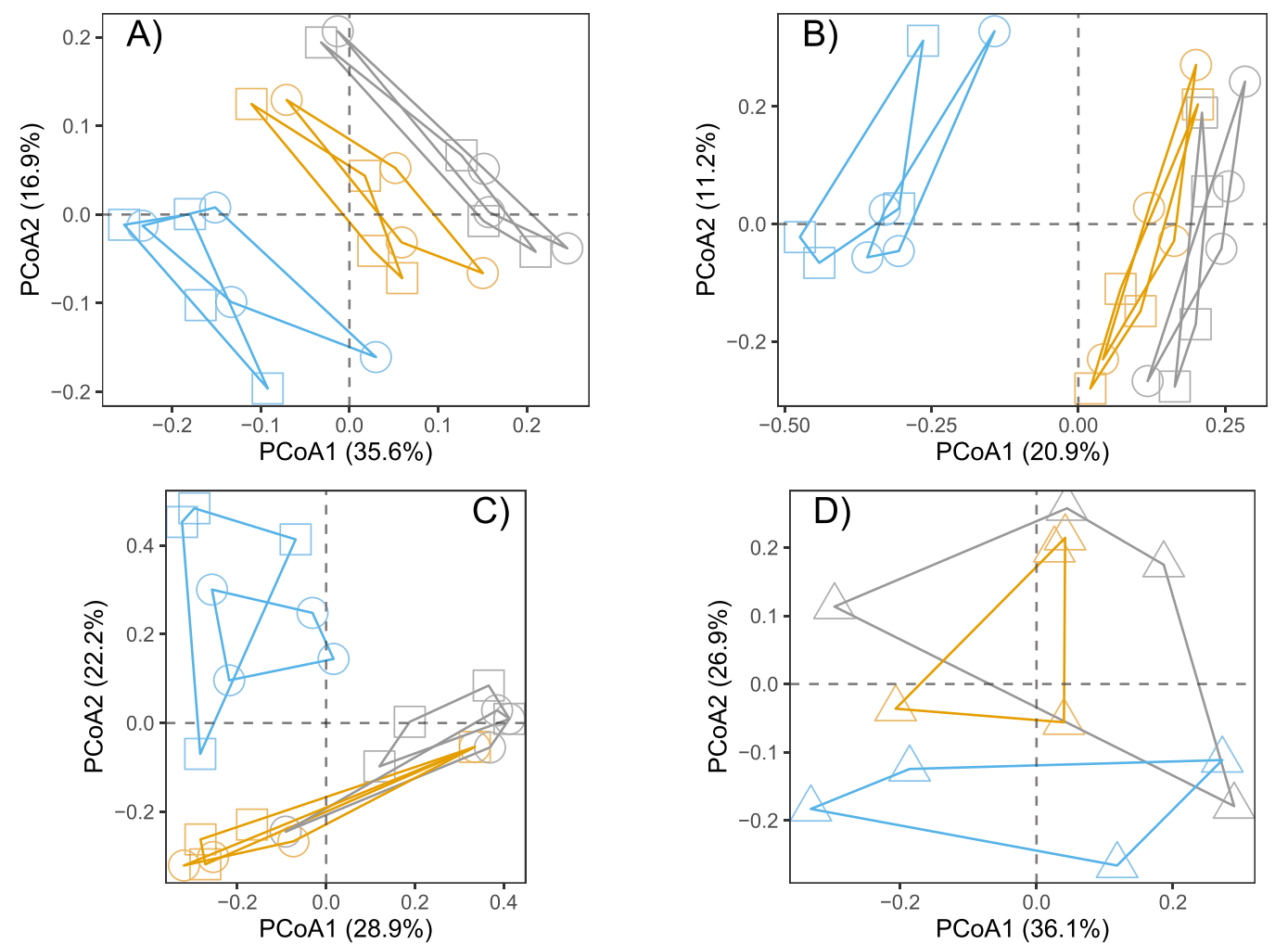
Fig. 1. Principal coordinates analysis (PCoA) of Bray-Curtis dissimilarities of A) bacterial, B) fungal, C) acarid, and D) nematode communities as affected by tillage: standard tillage (grey), minimum tillage (yellow) and no-tillage (blue) in two soil depths 0–10 cm (square) and 10–20 cm (circle) for bacteria, fungi and acari or in one soil depth 0–20 cm (triangle) for nematodes.

relative abundance when compared to ST and MT (Fig. A3). The cluster 3 contained particularly relatively abundant taxa. These were taxa such as a Rhizobium from the genus *Microvirga* from the family *Beijerinckiaceae* (Fig. A4), Actinobacteria from the family *Micromonosporaceae* (Fig. A5), Acidobacteria from the family *Blastocatellaceae* (Fig. A6), and Planctomycetes from the Isosphaerales (Fig. A7) and Tepidisphaerales (Fig. A8).

Bacteria with the highest relative abundance under ST, and/or MT were placed in clusters 1, 2, 4, and 5 (Fig. 2A). Particularly interesting in the context of plant responses was cluster 4 with significant enrichment of taxa from *Bacillus*, *Cohnella*, and *Streptomyces* under ST (Fig. A9 and A5).

Taking a look at fungal community structure derived from PCR amplified ITS2 barcoding, the most relatively abundant phyla in descending order were Ascomycota (44 %), Basidiomycota (25 %), Chytridiomycota (5 %), Mortierellomycota (4 %), Glomeromycota (3 %), Mucoromycota (1 %), and Monoblepharomycota (0.3 %) (Fig. A10). Further, more basal fungal clades were also detected in lower relative abundance such as Aphelidiomycota, Basidiobolomycota, Olpidiomycota, Rozellomycota, and Zoopagomycota (supplementary file A2).

Differential abundance analysis indicated that 51 fungal taxa were significantly associated with tillage and only one with depth (FDR<5 %). They represented a maximum of 32 % (NT, 0–10 cm) and a minimum of 8 % (MT, 0–10 cm) of the ITS2 sequences. The change profiles of fungi clustered into 6 informative groups (Fig. A11). Cluster 5, 1, and 2, in order of decreasing mean log-fold change, were associated with relative increases of taxa under NT. In particular, *Coprinellus curtus* (order Agaricales, phyl. Basidiomycota) in cluster 5 exhibited a strong enrichment in topsoil, increasing from 0.004 % under ST to 20.6 % under NT conditions (Fig. A12). Similarly, other Agaricales in cluster 1

and 2 including *Psathyrella* (fam. *Psathyrellaceae*), *Crepidotus* (fam. *Crepidotaceae*), and *Conocybe* (fam. *Bolbitiaceae*) increased under NT. Other taxa in cluster 5 were from the phylum Ascomycota and the classes Dothideomycetes (fam. *Didymosphaeriaceae* and *Phaeosphaeriacea*, Fig. A13) and Leotiomycetes (fam. *Sclerotiniaceae*, Fig. A14), amongst others. Clusters 3, 4, and 6 were characterized by strong relative decreases of fungi under NT (Fig. 2B). Particularly cluster 3 contained relatively abundant fungal taxa, such as *Zymoseptoria triticii* (Ascomycota, Fig. A13), *Aspergillus thesauricus* (Ascomycota, Fig. A15), *Udeniomyces* (Basidiomycota) and several unassigned Ascomycotan families. Cluster 4 was represented by taxa with strongest relative increases under MT, containing a taxon from the genus *Fusarium* (Ascomycota, Fig. A16), and further assigned taxa from the same class such as *Achaetomium*, and *Metacordyceps*.

3.3. Impact of tillage on soil functionality

Soil functionality was assessed by community level substrate utilization profiling (CLPP), potential enzymatic activity (EEA) of C, N, and P compounds, and calculations of C flow through the nematode community (Table 3). Tillage treatment significantly affected CLPP and EEA levels (p < 0.01). Values for CLPP were significantly higher in NT and MT vs. ST (p < 0.05), and for the former treatments it was also found that in top soil (0–10 cm) significantly higher values were measured vs. lower depth (10–20 cm). EEA of C, N, and P cycles was significantly higher in NT vs. MT and ST (p < 0.05). On average, NT exhibited in all soil functionality measures the highest values, except for the fungal mediated OM decomposition derived from nematode composition.
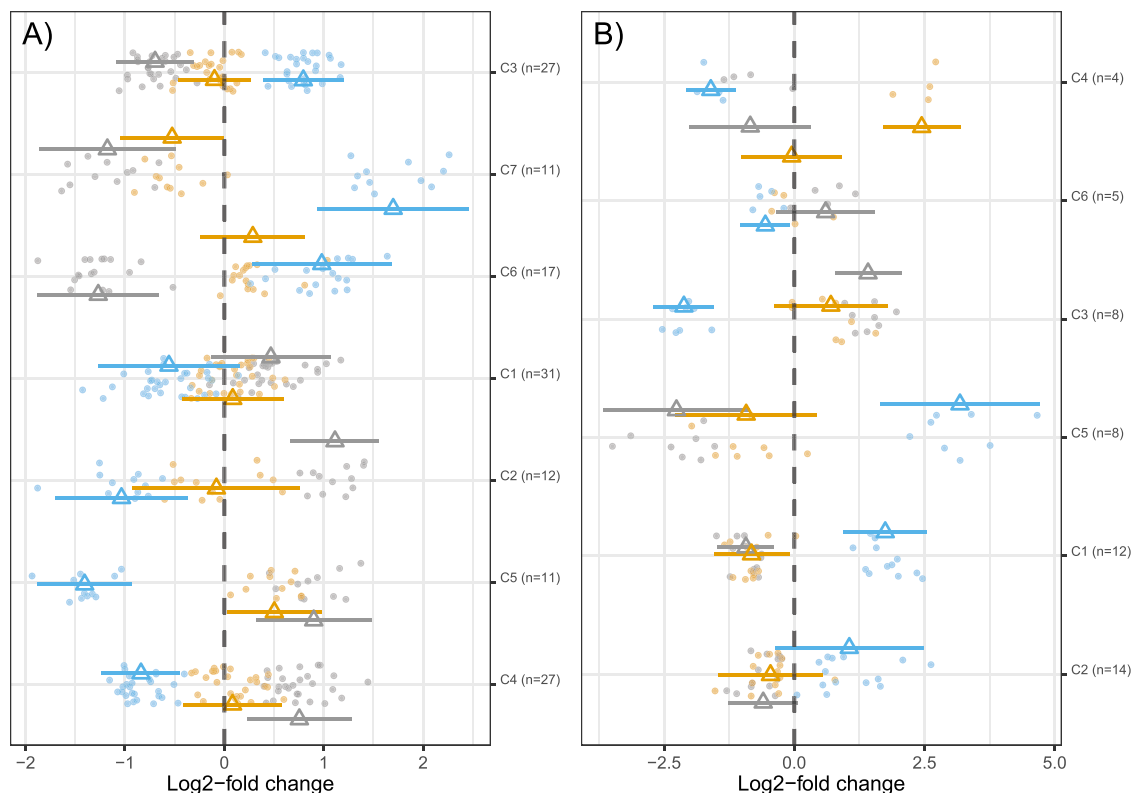
Fig. 2. Differentially abundant A) bacteria and B) fungi under standard tillage (grey), minimum tillage (yellow) and no-tillage (blue) treatment. Significantly differentially abundant bacterial OTUs (n = 136) and fungal OTUs (n = 51) were determined with LinDA at 5 % FDR. Shown are average log2-fold changes per taxon with tillage treatments against the global mean, averaging over depth. Clusters indicate number of taxa in that group and number of clusters were informed by Tibshirani criterion of the Gap statistic. For identities of taxa and clustering differences with Management, Depth and Plot see supplementary Fig. A37 and A63 for bacteria and fungi, respectively.

Table 3

Soil functionality assessed under standard tillage (ST), minimum tillage (MT) and no-tillage (NT) analyzed in 0–20 cm depth or individually in 0–10 cm and 10–20 cm. Soil functionality consists of indices for community level physiological profile (CLPP with basal respiration and cumulated multiple substrate induced respiration (MSIR)), extracellular enzymatic activity (EEA) involved in carbon (C, beta-glucosidase, cello-biohydrolase, xylosidase), nitrogen (N, N-acetyl-glucosidase, L-aminopeptides), and phosphorous (P, alkaline and neutral phosphatases) cycling, and nematode functional indices (enrichment metabolic footprint (EF), enrichment Index (EI), and channel Index (CI)). Values reported are estimated marginal means with 95 % confidence interval given in brackets. Model outputs are indicated with $p \leq 0.05$ * , 0.01 * * , 0.001 * ** . Different letters indicate significant differences between groups ($\alpha=0.05$).

	Tillage	Depth	Tillage:Depth	ST	MT	NT
CLPP (μg CO_2-C g^{-1} soil h^{-1})						
Basal respiration	$F_{2,9} = 8.9$ * *	$F_{1,9} = 1.8$	$F_{2,9} = 3.5$	0.4 [0.0, 0.8] b	0.9 [0.5, 1.2] ab	1.4 [1.0, 1.8] a
MSIR	$F_{2,10} = 12.6$ * *	$F_{1,9} = 1.7$	$F_{2,9} = 1.4$	5.0 [2.3, 7.7] b	8.7 [6.0, 11.4] b	13.0 [10.3, 15.7] a
SIR-MBC (μg C g^{-1} soil)	$F_{2,11} = 18.1$ * **	$F_{1,9} = 1.1$	$F_{2,9} = 1.4$	69 [32,106] c	129 [92,166] b	202 [165,239] a
Metabolic quotient, qCO_2, as basal respiration with spline MBC	$\chi^2= 0.5$	$\chi^2= 0.5$	$\chi^2= 5.4$	0.63 [0.22,1.04]	0.87 [0.71,1.02]	0.78 [0.50,1.06]
Metabolic quotient (nominal)				0.61	0.65	0.68
Extracellular enzymatic activity (nmol substrate g^{-1} soil h^{-1})						
C cycle	$F_{2,11} = 11.9$ * *	$F_{1,9} = 1.0$	$F_{2,9} = 0.1$	328 [87,568] b	542 [302,783] b	1069 [828. 1309] a
N cycle	$F_{2,14} = 26.5$ * **	$F_{1,9} = 0.9$	$F_{2,9} = 0.0$	132 [105,166] c	231 [184,291] b	450 [358,566] a
P cycle	$F_{2,10} = 6.8$ * *	$F_{1,9} = 2.4$	$F_{2,9} = 0.6$	73 [32,115] b	111 [70,152] ab	166 [125,207] a
Nematode functional indices (μg C kg^{-1} soil)						
EF: C mineralized by bacterial-feeding enrichment-opportunistic nematodes (μg C kg^{-1} soil)	$F_{2,8} = 0.7$	0–20 cm		80 [47,160]	100 [56,216]	131 [69,314]
EI: Organic matter (OM) decomposition mediated by bacterial channel	$F_{2,8} = 0.4$	0–20 cm		48 [25,71]	47 [24,70]	58 [35,81]
CI: OM decomposition mediated by fungal channel	$F_{2,8} = 0.4$	0–20 cm		50 [19,81]	43 [12,74]	34 [3,65]

3.4. Impact of tillage on wheat performance

At flowering stage, total aboveground biomass of individually weighed wheat plants was significantly affected by tillage ($p < 0.05$), decreasing from ST, over MT to NT by more than 2-fold (Table 4). This trend was seen alike when resolving for the compartments head, leaves and stem. The root biomass was not significantly different between tillage treatments at this growth stage ($p > 0.05$), however, on average, wheat under ST exhibited higher root biomass, followed by NT and lowest under MT (Table 4). The root:shoot ratio was significantly higher under NT compared to MT and ST ($p < 0.05$). The wheat root-to-soil interface was resolved further by characterizing root traits including number of root tips, branch points, total length/area/volume, diameter

of roots and root orientation (Table 4). Only root median diameter was significantly higher under NT compared to ST and MT ($p < 0.05$). Not significant, but on average higher under NT were also root average diameter, root maximum diameter and large (>0.2 mm) root diameter length. For wheat roots under ST, the number of root tips, root surface area and total root volume were on average highest. And for wheat roots under MT, number of root branch points, branching frequency, total root length, the proportion of root length in fine (<0.1 mm) and medium (0.1–0.2 mm) range diameter classes were on average highest, while root angle orientation was lowest (Table 4).

At harvest, wheat yields and thousand kernel weight were similar across treatments (Table 5). In contrast, grain N concentration (%) were significantly higher under ST compared to those of NT ($F_{2,6}=5.6$,

Table 4

Wheat growth performance at flowering stage in standard tillage (ST), minimum tillage (MT) and no-tillage (NT) systems. The aboveground parameters refer to individual plants collected from a circular area 9 cm in diameter and the corresponding root parameters from a depth of 20 cm. Values are estimated marginal with 95 % confidence interval given in brackets. Model output are indicated with $p \leq 0.05$ * , 0.01 * * , 0.001 * ** . Statistical analyses that failed ANOVA assumptions are reported in brackets. Different letters indicate significant differences between groups ($\alpha=0.05$).

Wheat growth parameter	Tillage	ST	MT	NT
Plant biomass (per cylinder area)				
Aboveground biomass (g)	($F_{2,6} = 5.1$ *)	27	15	11
Head (spike) biomass (g)	$F_{2,6} = 3.2$	9.0 [5.4, 18.7]	5.1 [3.5, 8.2]	4.6 [3.2, 7.3]
Leaf biomass (g)	$F_{2,6} = 6.4$ *	4.7 [2.8, 7.8] a	2.6 [1.5, 4.3] ab	1.6 [1.0, 2.7] b
Stem biomass (g)	($F_{2,6} = 6.5$ *)	13.7	7.6	4.9
Root biomass (g)	$F_{2,6} = 0.3$	0.86 [0.50, 1.21]	0.70 [0.35, 1.06]	0.80 [0.44, 1.15]
Root to shoot ratio	$F_{2,6} = 5.9$ *	0.03 [0.01, 0.05] b	0.04 [0.02, 0.06] b	0.07 [0.05, 0.09] a
Root system characteristics (per cylinder volume)				
Root tips (counts)	$F_{2,6} = 0.1$	51928 [20091,123600]	42006 [15908,101778]	44599 [16994,107515]
Root branch points (counts)	($F_{2,6} = 0.9$)	70995	79941	56659
Root branching frequency (freq. mm^{-1})	($F_{2,6} = 1.5$)	1.10	1.18	1.00
Root network area (mm^2)	$F_{2,6} = 0.0$	12906 [8345,17466]	12792 [8231,17352]	12247 [7686,16808]
Total root volume (mm^3)	$F_{2,6} = 0.1$	12272 [6303,18240]	10814 [4845,16783]	10530 [4561,16499]
Total root surface area (mm^2)	$F_{2,6} = 0.1$	69555 [42125,96925]	67592 [40192,94992]	62697 [35298,90097]
Total root length (mm)	($F_{2,6} = 0.6$)	65102	71601	56486
Root average diameter (mm)	($F_{2,6} = 11.5$ **)	0.34	0.29	0.35
Root median diameter (mm)	$F_{2,6} = 12.3$ * *	0.22 [0.21, 0.24] b	0.20 [0.18, 0.22] b	0.25 [0.24, 0.27] a
Root maximum diameter (mm)	$F_{2,6} = 0.8$	3.40 [2.74, 3.98]	3.42 [2.76, 4.00]	3.78 [3.17, 4.33]
Root length diameter range < 0.1 mm (mm)	$F_{2,6} = 1.2$	9114 [4922,18404]	11331 [5964,23665]	6401 [3597,12281]
Root length diameter range 0.1–0.2 mm (mm)	($F_{2,6} = 2.1$)	21762	24884	16159
Root length diameter range > 0.2 mm (mm)	$F_{2,6} = 0.0$	33207	33127	33299
Root crown analysis				
Average root orientation (°, deg.)	($F_{2,6} = 1.6$)	46.0°	43.9°	45.2°
Shallow angle frequency 0–30° (%)	$F_{2,6} = 1.6$	31.2 [27.1, 35.3]	35.4 [31.3, 39.5]	33.6 [29.5, 37.7]
Medium angle frequency 30–60° (%)	($F_{2,6} = 0.2$)	32.6	32.3	31.9
Steep angle frequency 60–90° (%)	($F_{2,6} = 1.5$)	35.1	32.0	34.2

Table 5

Wheat grain yield, nutritional and technological quality in standard tillage (ST), minimum tillage (MT) and no-tillage (NT) systems. Values presented are estimated marginal means with 95 % confidence interval given in brackets. Model output are indicated with $p \leq 0.05$ * , 0.01 * * , 0.001 * ** . Statistical analyses that failed DHARMa diagnostics are reported in brackets. Different letters indicate significant differences between groups (α=0.05).

	Tillage	ST	MT	NT
Harvest parameters				
Grain yield (dt ha^{-1})	$F_{2,6} = 0.8$	7.3 [4.8, 9.7]	5.5 [3.0, 7.9]	6.0 [3.6, 8.5]
Thousand kernel weight (g)	$F_{2,6} = 1.8$	17.1 [15.1, 19.1]	17.7 [15.7, 19.7]	19.3 [17.3, 21.3]
Nutrients				
C (g kg^{-1})	$F_{2,6} = 2.0$	430 [427,433]	429 [426,432]	427 [424,430]
N (g kg^{-1})	$F_{2,6} = 5.6$ *	31 [28,34] a	28 [25,31] ab	25 [22,28] b
S (g kg^{-1})	$F_{2,6} = 0.8$	1.8 [1.7, 2.0]	1.7 [1.5, 1.9]	1.7 [1.6, 1.9]
P (g kg^{-1})	($F_{2,6} = 0.8$)	4.06	3.88	3.92
K (g kg^{-1})	($F_{2,6} = 4.9$)	5.43	5.72	5.19
Mg (g kg^{-1})	$F_{2,6} = 1.2$	1.44 [1.33, 1.55]	1.40 [1.29, 1.51]	1.34 [1.23, 1.45]
Ca (mg kg^{-1})	($F_{2,6} = 12.9$ **)	493	923	410
Cl (mg kg^{-1})	$F_{2,6} = 4.4$	724 [613,835]	906 [795,1017]	768 [658,879]
Si (mg kg^{-1})	$F_{2,6} = 6.7$ *	191 [53,329] b	409 [271,547] a	131 [−7, 268] b
Fe (mg kg^{-1})	($F_{2,6} = 2.6$)	37	30	25
Mn (mg kg^{-1})	($F_{2,6} = 3.6$)	40	39	34
Zn (mg kg^{-1})	$F_{2,6} = 0.5$	30 [25,38]	28 [24,35]	27 [23,33]
Cu (mg kg^{-1})	$F_{2,6} = 0.8$	5.7 [5.1, 6.6]	5.3 [4.7, 6.0]	5.3 [4.7, 6.0]
Ni (mg kg^{-1})	$F_{2,6} = 1.3$	0.5 [0.4, 1.0]	0.4 [0.3, 0.6]	0.5 [0.3, 0.9]
Mo (mg kg^{-1})	$F_{2,6} = 0.9$	0.2 [0.0, 0.3]	0.1 [0.0, 0.3]	0.2 [0.1, 0.4]
Co (mg kg^{-1})	$F_{2,6} = 1.0$	0.03 [0.02, 0.05]	0.03 [0.01, 0.04]	0.04 [0.03, 0.06]
B vitamins				
Thiamine (B1) (mg kg^{-1})	$F_{2,6} = 12.5$ * *	6.4 [5.6, 7.6] a	4.7 [4.2, 5.3] b	4.5 [4.1, 5.1] b
Riboflavin (B2) (mg kg^{-1})	$F_{2,6} = 6.3$ *	1.1 [0.9, 1.3] a	0.8 [0.6, 1.0] b	0.7 [0.5, 0.9] b
Niacine (B3) (mg kg^{-1})	($F_{2,6} = 2.3$)	14.6	12.1	11.3
Pantothenic acid (B5) (mg kg^{-1})	($F_{2,6} = 5.5$ *)	9.1	7.6	6.3
Pyridoxine (B6) (mg kg^{-1})	($F_{2,6} = 6.9$ *)	2.9	2.2	2.1
Folate (B9) (mg kg^{-1})	$F_{2,6} = 4.6$	0.6 [0.5, 0.7]	0.4 [0.3, 0.5]	0.4 [0.3, 0.5]
Technological properties				
A-type starch (>10 µm) (%)	$F_{2,6} = 11.2$ * *	93.0 [91.5, 94.5] a	91.3 [89.9, 92.8] a	89.0 [87.5, 90.5] b
B-type starch (2–10 µm) (%)	($F_{2,6} = 11.6$ **)	6.9	8.6	10.9
C-type starch (< 2 µm) (%)	$F_{2,6} = 0.4$	0.0 [0.0, 0.1]	0.0 [0.0, 0.1]	0.1 [0.0, 0.1] b
Glutenins (%)	$F_{2,6} = 3.7$	1.38 [1.19, 1.56]	1.14 [0.96, 1.33]	1.11 [0.92, 1.29]
Gliadins (%)	$F_{2,6} = 4.0$	0.67 [0.55, 0.80]	0.63 [0.50, 0.76]	0.47 [0.35, 0.60]

$p < 0.05$, Table 5). In correspondence to the highest N content in grains grown under ST, the grain B vitamin content for Thiamine (B1) and Riboflavin (B2) were found to be significantly highest under ST compared to NT and MT. Interestingly, grain Ca and Si contents were significantly highest in wheat grown under MT, while other macronutrients such as C, P, K, S, Mg and micronutrients did not differ between tillage treatments. Regarding technological grain properties, also the distribution of starch size classes significantly differed between treatments with a higher abundance of A-type starches (>10 µm) in ST compared to NT ($p < 0.01$) and a higher abundance of B-type starches (2 <x < 10 µm) in NT compared to ST ($p < 0.01$) (Table 5). In contrast, the abundance of gliadins and glutenins was similar across treatments (Table 5).

4. Discussion

4.1. Reducing tillage intensity enhanced soil chemical and biological properties

The increases in total soil C, N, P, and K under NT are consistent with previously reported results of increased organic matter measures from the same field experiment (Martin-Rueda et al., 2007, Martín-Lammerding et al., 2013, 2011), as well as the results of the meta-study by Haddaway et al. (2017).

Unexpectedly, the soil moisture content in NT was the lowest (Table 1). This was not reported in previous studies from the same site, where NT exhibited higher soil water content at flowering stage. Indeed, it was argued that less intensive tillage practices are also water saving practices (Santin-Montanya et al., 2020). Further, a higher organic matter content would in principle enable higher water holding capacity

from aggregate formation and pore space. The differing water status under NT in this study could derive from temporal water dynamics in connection with sampling time. For example, the precipitation deficit together with increased temperatures in April to June 2022 (Table A1) could have led to high evaporation and with differing vegetation cover in the tillage treatments differing transpiration rates depleting the soil water supply and leading to potential drought conditions. Co-occurring plants (e.g. weeds) in tillage treatments were found to influence soil water status by complex interactions with seasonal total rainfall, legacy effects over years, and with short-term weather/sampling time (Gandia et al., 2021; Santin-Montanya et al., 2020).

Corresponding to the higher C content in NT, our results showed increased abundances of prokaryotic and eukaryotic gene copies, and on average an increase in acari and nematodes (Table 2) as well as higher SIR microbial biomass (Table 3). In addition, we observed higher basal respiration, substrate utilization rates and enzymatic activities under NT (Table 3), which are indicators for higher microbial biomass. Our results are consistent with the meta-analysis of Chen et al. (2020) who found a positive effect of reduced tillage on the abundance of bacteria and fungi as well as an increase in total C and N that might be linked with the increase of SOC under NT (Lori et al., 2017). Similarly, a positive association of soil biological indicators with decreasing tillage intensity was observed in the meta-analysis of Nunes et al. (2020). However, despite that MT exhibited similar prokaryotic and eukaryotic gene copies to NT, the functional activity levels were significantly lower (Table 3). This could result from significantly different bacterial and fungal microbial communities (Fig. 1, Fig. 2), that would be expected to result in different functionalities and activity levels. Indeed, a previous study from the same field experiment showed an increase in soil basal respiration, microbial biomass C and β-glucosidase activity under NT

(Martín-Lammerding et al., 2015). The observed increased in eukaryotic:prokaryotic qPCR gene copy ratio (Table 2) from ST, over MT, to NT is consistent with findings that less intensive tillage practices are resulting in increased total microbial biomass and fungal proportions (Six et al., 2006; Piazza et al., 2019). In contrast, van Groenigen et al. (2010) and Murugan et al. (2014) did not find a change in the proportion of bacteria and fungi under minimum tillage, but an increase in saprotrophic fungi, which is in line with the increase in relative abundance of taxa with saprotrophic/seed nutrition under NT observed in this study (discussed in Section 4.3). The studies of van Groenigen et al. (2010) and Murugan et al. (2014) highlighted the importance of differing organic matter degrading capabilities of fungal groups and that this can have an effect on the organic matter dynamics. An increased proportion of fungal decomposers could also be an alternative explanation, apart from stress and disturbance (Wardle and Ghani, 1995, Anderson and Domsch, 2010), for the here observed increase of the metabolic quotient from ST, over MT, to NT (Table 3).

4.2. Tillage intensity shapes soil biota community structure

As hypothesized, tillage intensity significantly shaped bacterial, fungal, and acarid communities, while this could not be shown for nematodes (Fig. 1, Table A2). Largely this is consistent with previous studies documenting differences in the community structures of microorganisms (Hartmann et al., 2018; Kraut-Cohen et al., 2020; Orrù et al., 2021; Wang et al., 2020), nematode (Puissant et al., 2021), and acari (Betancur-Corredor et al., 2022) between ploughed, minimum tillage, and no-tillage systems. A key factor driving these differences may be the increase in SOC with minimum tillage intensity and the associated increase in microbial community size and activity (Lori et al., 2017; Ramírez et al., 2020). Moreover, tillage intensity has been demonstrated to impact various soil properties, including the stability and size of aggregates and bulk density (Li et al., 2019; Nunes et al., 2020; Mondal and Chakraborty, 2022). These properties are also influenced by soil microbes, which in turn might shape the other soil community by bottom-up forces (Hartmann and Six, 2023; Philippot et al., 2024). Since tillage intensity affects numerous relative abundance changes at the microbial level, even contrasting within families and genera, an extensive ecological description of bacterial and fungal clades with changes under tillage intensities can be found in the supplementary (supplementary data 1.1.1 for bacteria and 1.4.1 for fungi). From a biological standpoint, these findings align with ecological theory. Tillage-induced changes in nutrient availability (quality and quantity of organic matter, root traits) and further soil properties lead to shifts in multidimensional niche space. Indeed, the competitive exclusion principle states that if two species use the exact same resources, the one using the resources more efficiently will exclude the other (Gause, 1934). Therefore, coexistence of such a high number of bacterial and fungal taxa (hundreds to thousands) found on a small volume that DNA was extracted from, and with many taxa using similar resources is only possible, if substantial niche differences evolve between closely related taxa or taxa using similar resources (the multidimensional niche: Hutchinson, 1959). Of these niche dimensions a high degree of micro-spatial separation and environmental variability could play a role (Horner-Devine et al., 2004). Indeed, high resolution of soil bacterial translational dynamics have shown that competition within nutritional guilds was strongest and affected by specialist-directed nutritional substances and abundance of competitors (Moyne et al., 2023). For a more in-depth discussion, we will focus on two key aspects: the formation of soil biocrust (explained later) under NT and the dynamics of fungal plant pathogens and fungal antagonists.

Under NT, the most pronounced gene copy increase in bacteria was from a taxon in the *Tychonema* genus (a Cyanobacterium) (Fig. 2A, cluster 7). This taxon assignment is monophyletic with *Microcoleus vaginatus* (Strunecky et al., 2023; Zhang et al., 2016), which are well described for their importance to soil biocrust formation (Büdel, 2005;

Powell et al., 2015). Given the increase in total 16S gene copies under NT (Table 2), the increase in cyanobacteria may hint at their role in soil C and N accumulation (Table 1). This could contribute to soil biocrust formation, a less studied aspect in arable farming. Biological soil crusts are linkages of mineral soil particles with a community of photo-autotrophic cyanobacteria, algae, lichens, bryophytes, and associated heterotrophic fungi and prokaryotes that often develop in arid regions or on early habitats such as rocks. The organismal composition is structured by local degree of abiotic stresses such as aridity and solar radiation (Büdel, 2005; Grishkan et al., 2019; Hu and Satten, 2023). In arable farming, where the soil surface is often disturbed and exposed when bare, particularly in semi-arid regions, the pioneering role of biocrusts and microbial photoautotrophs is interesting in regard to their reported contributions to SOM built-up, N_2-fixation, and climate resilience (Grishkan et al., 2019; Powell et al., 2015; Madigan et al., 2021; Büdel, 2005; Hu and Satten, 2023; Mazor et al., 1996). Besides *Tychonema*, we also detected other cyanobacteria some associated to lichens or algae (from the order Chaetothyriales such as *Bradymyces*, *Exophiala*, Lücking et al., 2009), as well as micro-fungal and bacterial heterotrophs that were reported to occur in soil biocrusts (supplementary data 1.13). Thus, our results suggest that the development of biocrusts is possible under NT, whereas ST and MT might exhibit a "critical" degree of disturbance (Fig. A17).

Focusing on fungal pathogen – antagonist interactions, we observed a relative decrease of two fungal plant pathogens, *Zymoseptoria tricii* (Ascomycota, class Dothideomycetes, Quaedvlieg et al., 2011) and a *Fusarium* sp. (Ascomycota, class Sordariomycetes, Lombard et al., 2015) under NT compared to ST (clusters 3 and 4 in Fig. 2B). In contrast, other organisms in the class Dothideomycetes relatively increased under NT including *Spegazzinia radermacherae,* a saprotroph living on fallen seed pods (Jayasiri et al., 2019) and *Sclerostagonospora*, a pathogen or saprotroph of various monocotyledons and dicotyledons (Phookamsak et al., 2014) as well as other saprotrophs including *Keissleriella* (*cirsii*) and *Clarireedia bennettii* (class Leotiomycetes), the latter known as pathogen of C3 turfgrasses (Salgado-Salazar et al., 2018). The increase of some fungal plant saprotrophs and seed/pollen attacking taxa under NT might have resulted from an increased frequency of co-occurring weeds, weed richness, and weed seed bank density observed in soil under MT and NT (Santín-Montanyá et al., 2020, 2018, 2016). The increase of herbivore nematodes under NT (Table 2) supports this assumption.

On the flipside, the most notable fungal plant pathogen antagonist strongly increased under NT was a *Coprinellus curtus* (cluster 5, Fig. 2, Fig. A12). As a saprotroph, *C. curtus* could be expected to grow well at higher OM levels under NT. In addition, a relevant agricultural isolate of *C. curtus* showed antagonistic behavior against several plant pathogens including *Fusarium oxysporum* and *Rhizoctonia solani* (Nakasaki et al., 2007), which might explain the observed decrease of *Fusarium* sp. in the present study. A multifunctionality of other OM-degrading Basidiomycetes that relatively increased under NT, such as *Psathyrella*, *Crepidotus*, and *Conocybe*, may be their plant pathogen suppressive effect, either by direct interference or by indirect competition. It is speculated here that higher OM levels under NT may allow these fungi to thrive.

4.3. Impaired wheat growth and nutritional quality under low intensity tillage under drought conditions despite enhanced soil biological indicators

Wheat growth, average wheat yields, and the nutritional quality indicators grain N content and grain vitamin thiamine (B1) and riboflavin (B2) levels, were highest under ST and lowest under NT (Table 5). Potential drought conditions in April to June 2022 might have hampered yields in all tillage treatments when compared to higher wheat yields in 2021 and 2023 (Table A1). This suggests that soil water availability appeared to be the limiting factor in 2022, leading to reduced yields in all tillage treatments. With differential vertical soil stratification resulting from the tillage treatments and different soil

cover (Sections 4.1, 4.2), differences in evapotranspiration rates likely contributed to variations in soil water availability. This may further explain wheat performance across tillage treatments in 2022. Our findings are consistent with the meta-analysis by Pittelkow et al. (2015), who reported increased wheat yield and N uptake under more intensive tillage practices. As N is a crucial element in the synthesis of proteins and enzymes involved in the production of B vitamins, it was expected that vitamin B levels would show similar patterns, directly correlating with grain N content. In addition, studies have demonstrated that B vitamins are differentially affected by genotype and environmental factors such as temperature, precipitation, and soil conditions (Shewry et al., 2011; Batifoulier et al., 2006). These factors may further explain the observed differences in B vitamin levels induced by tillage practices. In addition, this is the first study reporting about tillage-induced changes in wheat technological properties as reflected by a shift in A- and B-type starch distribution and on average higher content of Gliadins and Glutenins under ST. As recently reviewed by Guo et al. (2023) the distribution of A- and B-type starch are important technological quality indicators as they strongly influence the quality of dough and final products.

Explanations for wheat performance may partly trace to root system architecture measured at the flowering stage and partly overlapping with the onset of drought conditions in April to June 2022. The roots data (Table 4) showed that the root-to-shoot ratio was highest under NT, indicating resource allocation for soil penetration and root thickening in wheat in compacted soils (Muñoz-Romero et al., 2010; Watt et al., 2005). Indeed, wheat roots under NT had the significantly highest median root diameter, and on average higher root average diameter, root maximum diameter, and larger root diameter, which were consistent with descriptions of soil compaction effects on wheat (Muñoz-Romero et al., 2010; Atwell, 1990; Watt et al., 2005). The better performance of wheat under ST is reflected by the characteristics of its root system with an increase in root area, root volume and the number of root tips (Table 4). These characteristics, in turn, are reported to be linked to higher N mineralization potential through: 1) root exudation associated with number of actively growing root tips, considered as hot spots of microbial abundance and activity in the rhizosphere, 2) root surface or length being indicative of the potential for nutrient exploration and establishment of biological associations, and 3) proportion of fine roots influencing the water uptake capacity and the total root surface (Freschet et al., 2021, Delaplace et al., 2015, Kuzyakov and Blagodatskaya, 2015, Watt et al., 2009, Watt et al., 2008, McCully, 1999). Roots influence microbes and their nutrient mobilization potential by supplying energy in what is summarized as the "Rhizosphere effect" (Kuzyakov and Blagodatskaya, 2015, Nguyen, 2009, Hodge et al., 2000). This could explain the significantly higher proportion of rhizosphere-associated or potentially plant growth promoting taxa under ST of *Bacillus* and *Cohnella* (Firmicutes) (Madigan et al., 2021, Gupta et al., 2020, Khianngam et al., 2010), and Actinomycetes such as *Streptomyces* and *Luedemanella* (Carro et al., 2018, Madigan et al., 2021, Ara and Kudo, 2007). It is also important to mention the more pronounced drought during the study year compared to previous years (Table A1). The higher proportion of fine roots may have contributed to increased water and N uptake, resulting in higher wheat yields under ST.

Wheat grown under MT did not perform as well in regards to grain yield and quality as wheat grown under ST (Table 5). In the former, root traits were characterized by on average highest values for root branch points, branching frequency, and lowest root angle orientation with higher frequency of shallow angled roots (Table 4). Considering that MT only loosens the soil to a depth of about 15 cm, could mean easier soil penetration during the early growth stages of wheat, and negative effects during later growth stages associated with a soil compaction layer. At the same time, the root angle influences the vertical distribution of the roots (and their water uptake potential in deeper soil layers), which is influenced by soil compaction and could affect later wheat growth (Freschet et al., 2021, Delaplace et al., 2015, Watt et al., 2009, Watt et al., 2008, Watt et al., 2005). Sampling throughout the growing season

as done in Muñoz-Romero et al. (2010) for the comparison of NT versus ST could clarify whether the intermediate growth of wheat under MT is due to early growth promotion by easy soil penetration and later growth inhibition by soil compaction. In addition, legacy effects of long-term NT/MT on root characteristics might differ to conditions with recent/alternating tillage management practices.

Despite higher concentration of available soil nutrients (Table 1), increased abundances of prokaryotes, eukaryotes, nematodes and acari (Table 2), substrate mineralization potential and enzyme cycling activity under NT (i.e. N cycling, Table 3), wheat performance was lower than under ST (Table 4, Table 5). This is striking as the action of microbial grazers as well as the diurnal cycles of water uptake in the rhizosphere should liberate nutrients from the microbial pool for plant uptake (Drinkwater and Snapp, 2007; Clarholm, 1985) enhancing nutrient uptake under NT. Thus, other factors such as nutrient competition by higher weed pressure, microbial immobilization and/or slower SOM mineralization resulting in a reduced N availability or uptake might have limited wheat growth and grain N content in less intensive tillage systems (Cooper et al., 2016; Hofmeijer et al., 2019; Kuzyakov and Blagodatskaya, 2015; Nguyen, 2009; Hodge et al., 2000). Additionally, the impact of drought conditions in April to June 2022 (Table A1), might have shown water to be the most limiting factor and with additional bio-organic mass under NT (Sections 4.1, 4.2), its higher transpiration potential might have relatively reduced water status further. Here we have outlined possible physical and biological reasons for the decrease in wheat performance under reduced soil tillage intensity, however, the exact causes require further research.

5. Conclusion

Our study highlights the important role of tillage in shaping soil biodiversity and functionality. Varying tillage intensity is reflected in distinct shifts in both the structural and functional communities within the soil. Our findings provide evidence that the formation of biocrusts under NT may contribute to the accumulation of OM in upper soil layers. The lower growth performance and nutritional quality of wheat grains, despite enhanced soil chemistry and biology, points to underlying root structure problems that might have limited wheat growth and nutrient uptake. Addressing these issues may require the application of additional measures such as the cultivation of deep rooting inter-crops or complementary tillage practices to improve wheat production under no-tillage conditions. Alternatively, research into wheat varieties with root systems adapted to no-tillage conditions may offer promising solutions. In addition, the study showed that tillage intensity has the potential to alter technological grain properties and should be considered in the subsequent use of the wheat for production.

CRediT authorship contribution statement

Verlinde Thomas: Resources, Investigation. **Michel Jennifer:** Writing – review & editing, Supervision, Resources, Project administration, Methodology, Investigation, Formal analysis, Data curation, Conceptualization. **Van Der Straeten Dominique:** Writing – review & editing, Supervision, Resources, Project administration, Funding acquisition, Conceptualization. **Waibel Matthias:** Writing – review & editing, Writing – original draft, Visualization, Resources, Methodology, Formal analysis, Data curation. **Moya-Laraño Jordi:** Writing – review & editing, Supervision, Resources, Project administration, Investigation, Funding acquisition. **Balanzategui-Guijarro Iñaki:** Resources, Methodology, Investigation, Data curation. **Weinmann Markus:** Resources, Project administration, Investigation, Funding acquisition. **Antoine Maurine:** Resources, Methodology, Investigation. **Sanchez-Moreno Sara:** Writing – review & editing, Resources, Project administration, Methodology, Investigation, Formal analysis. **Delaplace Pierre:** Writing – review & editing, Supervision, Project administration, Funding acquisition, Conceptualization. **Perrochon Sibille:** Resources,

Investigation. **Cao Da:** Writing – review & editing, Resources, Methodology, Investigation, Formal analysis, Data curation. **Alvarez David:** Resources, Methodology, Investigation. **Santin-Montaña Inés:** Resources, Investigation. **Le Gouis Jacques:** Writing – review & editing, Supervision, Resources, Project administration, Funding acquisition, Data curation. **Tenorio José Luis:** Resources, Investigation. **Léon Claire:** Resources, Methodology, Investigation. **Thonar Cécile:** Supervision, Resources, Project administration, Funding acquisition. **Vanderschuren Hervé:** Writing – review & editing, Resources, Project administration, Funding acquisition. **Symanczik Sarah:** Writing – review & editing, Writing – original draft, Supervision, Resources, Project administration, Methodology, Funding acquisition, Conceptualization. **Manfroy Sandy:** Resources, Investigation.

Declaration of Competing Interest

The authors declare that they have no known competing financial interests or personal relationships that could have appeared to influence the work reported in this paper.

Acknowledgments

Appendix A. Supporting information

Supplementary data associated with this article can be found in the online version at doi:10.1016/j.agee.2025.109675.

Data availability

The microbiome data presented in the study are deposited in the NCBI Sequence Read Archive (SRA) repository, accession number PRJNA1198325 and PRJNA1198337. All other data are available on Zenodo (https://doi.org/10.5281/zenodo.15007358).

References

Akalin, A., 2020. Computational Genomics with R. CRC Press.

Anderson, M.J., 2006. Distance-based tests for homogeneity of multivariate dispersions. Biometrics 62 (1), 245–253.

Anderson, J.P., Domsch, K.H., 1978. A physiological method for the quantitative measurement of microbial biomass in soils. Soil Biol. Biochem. 10 (3), 215–221.

Anderson, T.H., Domsch, K.H., 2010. Soil microbial biomass: the eco-physiological approach. Soil Biol. Biochem. 42 (12), 2039–2043.

Ara, I., Kudo, T., 2007. Luedemannella gen. nov., a new member of the family Micromonosporaceae and description of Luedemannella helvata sp. nov. and Luedemannella flava sp. nov. J. Gen. Appl. Microbiol. 53 (1), 39–51.

Atwell, B.J., 1990. The effect of soil compaction on wheat during early tillering: I. Growth, development and root structure. New Phytol. 115 (1), 29–35.

Auguie, B., 2017. gridExtra: Miscellaneous Functions forGrid" Graph. R. Package Version 2.3⟨https://CRAN.R-project.org/package=gridExtra⟩.

Barker, K.R., 1985. Nematode extraction and bioassays. In: Barker, In.K.R., Carter, C.C., Sasser, J.N. (Eds.), An Advanced Treatise on Meloidogyne, Methodology, 2. North Carolina State University Graphics, Raleigh, N.C., N.C., pp. 19–35, 19–35.

Bates, D., Maechler, M., Bolker, B., Walker, S., 2015. Fitting linear mixed-effects models using lme4. J. Stat. Softw. 67 (1), 1–48. https://doi.org/10.18637/jss.v067.i01.

Batifoulier, F., Verny, M.A., Chanliaud, E., Rémésy, C., Demigné, C., 2006. Variability of B vitamin concentrations in wheat grain, milling fractions and bread products. Eur. J. Agron. 25 (2), 163–169.

Bell, C.W., Fricks, B.E., Rocca, J.D., Steinweg, J.M., McMahon, S.K., Wallenstein, M.D., 2013. High-throughput fluorometric measurement of potential soil extracellular enzyme activities. J. Vis. Exp. (81), e50961

Bender, S.F., Schulz, S., Martínez-Cuesta, R., Laughlin, R.J., Kublik, S., Pfeiffer-Zakharova, K., Vestergaard, G., Hartman, K., Parladé, E., Römbke, J., 2023. Simplification of soil biota communities impairs nutrient recycling and enhances above-and belowground nitrogen losses. New Phytol. 240, 2020–2034.

Betancur-Corredor, B., Lang, B., Russell, D.J., 2022. Reducing tillage intensity benefits the soil micro-and mesofauna in a global meta-analysis. Eur. J. Soil Sci. 73 (6), e13321.

Bongers, T., 1990. The maturity index: an ecological measure of environmental disturbance based on nematode species composition. Oecologia 83, 14–19.

Bray, J.R., Curtis, J.T., 1957. An ordination of the upland forest communities of southern Wisconsin. Ecol. Monogr. 27 (4), 326–349.

Brévault, T., Bikay, S., Maldes, J.M., Naudin, K., 2007. Impact of a no-till with mulch soil management strategy on soil macrofauna communities in a cotton cropping system. Soil Tillage Res. 97 (2), 140–149.

Brooks, M.E., Kristensen, K., van, Benthem, K.J., Magnusson, A., Berg, C.W., Nielsen, A., Skaug, H.J., Maechler, M., Bolker, B.M., 2017. glmmTMB balances speed and flexibility among packages for zero-inflated generalized linear mixed modeling. R. J. 9 (2), 378–400. https://doi.org/10.32614/RJ-2017-066.

Büdel, B., 2005. Microorganisms of Biological Crusts on Soil Surfaces. In: Buscot, F., Varma, A. (Eds.), *Microorganisms in Soils: Roles in Genesis and Functions*. Springer.

Cameron, C., 2007. MicroResp™ Technical Manual—A Versatile Soil Respiration System. Macaulay Institute, Craigiebuckler, Aberdeen, Scotland, UK.

Campbell, C.D., Chapman, S.J., Cameron, C.M., Davidson, M.S., Potts, J.M., 2003. A rapid microtiter plate method to measure carbon dioxide evolved from carbon substrate amendments so as to determine the physiological profiles of soil microbial communities by using whole soil. Appl. Environ. Microbiol. 69 (6), 3593–3599.

Cao, D., Heughebaert, L., Boffel, L., Stove, C., Van Der Straeten, D., 2024. Simultaneous quantification of seven B vitamins from wheat grains using UHPLC-MS/MS. Food Chem. 453, 139667.

Carro, L., Nouioui, I., Sangal, V., Meier-Kolthoff, J.P., Trujillo, M.E., Montero-Calasanz, M.D.C., Sahin, N., Smith, D.L., Kim, K.E., Peluso, P., Deshpande, S., Woyke, T., Shapiro, N., Kyrpides, N.C., Klenk, H.-P., Göker, M., Goodfellow, M., 2018. Genome-based classification of micromonosporae with a focus on their biotechnological and ecological potential. Sci. Rep. 8 (1), 525.

Chen, H., Dai, Z., Veach, A.M., Zheng, J., Xu, J., Schadt, C.W., 2020. Global meta-analyses show that conservation tillage practices promote soil fungal and bacterial biomass. Agric. Ecosyst. Environ. 293, 106841.

Clarholm, M., 1985. Interactions of bacteria, protozoa and plants leading to mineralization of soil nitrogen. Soil Biol. Biochem. 17 (2), 181–187.

Cooper, J., Baranski, M., Stewart, G., Nobel-de Lange, M., Bàrberi, P., Fließbach, A., Peigné, J., Berner, A., Brock, C., Casagrande, M., 2016. Shallow non-inversion tillage in organic farming maintains crop yields and increases soil C stocks: a meta-analysis. Agron. Sustain. Dev. 36, 1–20.

Creamer, R.E., Stone, D., Berry, P., Kuiper, I., 2016. Measuring respiration profiles of soil microbial communities across Europe using MicroResp™ method. Appl. Soil Ecol. 97, 36–43.

Dai, Z.W., Plessis, A., Vincent, J., Duchateau, N., Besson, A., Dardevet, M., Prodhomme, D., Gibon, Y., Hilbert, G., Pailloux, M., Ravel, C., Martre, P., 2015. Transcriptional and metabolic alternations rebalance wheat grain storage protein accumulation under variable nitrogen and sulfur supply. Plant J. 83, 326–343.

de Graaff, M.-A., Hornslein, N., Throop, H.L., Kardol, P., van Diepen, L.T., 2019. Effects of agricultural intensification on soil biodiversity and implications for ecosystem functioning: a meta-analysis. Adv. Agron. 155, 1–44.

Delaplace, P., Delory, B.M., Baudson, C., Mendaluk-Saunier de Cazenave, M., Spaepen, S., Varin, S., Brostaux, Y., du Jardin, P., 2015. Influence of rhizobacterial volatiles on the root system architecture and the production and allocation of biomass in the model grass Brachypodium distachyon (L.) P. Beauv. BMC Plant Biol. 15, 1–15.

Delgado-Baquerizo, M., Guerra, C.A., Cano-Díaz, C., Egidi, E., Wang, J.T., Eisenhauer, N., Maestre, F.T., 2020. The proportion of soil-borne pathogens increases with warming at the global scale. Nat. Clim. Change 10 (6), 550–554.

Delgado-Baquerizo, M., Grinyer, J., Reich, P.B., Singh, B.K., 2016. Relative importance of soil properties and microbial community for soil functionality: insights from a microbial swap experiment. Funct. Ecol. 30, 1862–1873.

Drinkwater, L.E., Snapp, S.S., 2007. Understanding and managing the rhizosphere in agroecosystems. In: Cardon, Z.G., Whitbeck, J.L. (Eds.), The Rhizosphere: An Ecological Perspective. Academic Press, pp. 127–153.

Edwards, M.A., Osborne, B.G., Henry, R.Jm., 2008. Effect of endosperm starch granule size distribution on milling yield in hard wheat. J. Cereal Sci. 48, 180–192.

Essel, E., Xie, J., Deng, C., Peng, Z., Wang, J., Shen, J., Xie, J., Coulter, J.A., Li, L., 2019. Bacterial and fungal diversity in rhizosphere and bulk soil under different long-term tillage and cereal/legume rotation. Soil Tillage Res. 194, 104302.

Ferris, H., 2010. Form and function: Metabolic footprints of nematodes in the soil food web. Eur. J. Soil Biol. 46 (2), 97–104.

Ferris, H., Bongers, T., de Goede, R.G.M., 2001. A framework for soil food web diagnostics: extension of the nematode faunal analysis concept. Appl. Soil Ecol. 18, 13–29.

Fox J., Weisberg, S., 2019. An R Companion to Applied Regression, Third edition. Sage, Thousand Oaks CA. <⟨https://socialsciences.mcmaster.ca/jfox/Books/Companion/⟩> .

Freschet, G.T., Roumet, C., Comas, L.H., Weemstra, M., Bengough, A.G., Rewald, B., Bardgett, R.D., De Deyn, G.B., Johnson, D., Klimesova, J., Lukac, M., McCormack, M. L., Meier, I.C., Pages, L., Poorter, H., Prieto, I., Wurzburger, N., Zadworny, M., Bagniewska-Zadworna, A., m, Blancaflor, E.B., Brunner, I., Gessler, A., Hobbie, S.E., Iversen, C.M., Mommer, L., Picon-Cochard, C., Postma, J.A., Rose, L., Ryser, P., Scherer-Lorenzen, M., Soudzilovskaia, N.A., Sun, T., Valverde-Barrantes, O.J., Weigelt, A., York, L.M., Stokes, A., 2021. Root traits as drivers of plant and ecosystem functioning: current understanding, pitfalls and future research needs. N. Phytol. 232 (3), 1123–1158.

Frey, B., Rime, T., Phillips, M., Stierli, B., Hajdas, I., Widmer, F., Hartmann, M., 2016. Microbial diversity in European alpine permafrost and active layers. FEMS Microbiol. Ecol. 92 (3), fiw018.

Gandía, M.L., Del Monte, J.P., Tenorio, J.L., Santín-Montanyá, M.I., 2021. The influence of rainfall and tillage on wheat yield parameters and weed population in monoculture versus rotation systems. Sci. Rep. 11 (1), 22138.

Gause, G. F., 1934. Competitive exclusion principle.

Gloor, G.B., Macklaim, J.M., Pawlowsky-Glahn, V., Egozcue, J.J., 2017. Microbiome datasets are compositional: and this is not optional. Front. Microbiol. 8, 2224.

Grishkan, I., Lázaro, R., Kidron, G.J., 2019. Cultured microfugal communities in biological soil crusts and bare soils at the Tabernas Desert, Spain. Soil Syst. 3 (2), 36.

Guardia, G., Tellez-Rio, A., García-Marco, S., Martin-Lammerding, D., Tenorio, J.L., Ibáñez, M.Á., Vallejo, A., 2016. Effect of tillage and crop (cereal versus legume) on greenhouse gas emissions and Global Warming Potential in a non-irrigated Mediterranean field. Agric. Ecosyst. Environ. 221, 187–197.

Guo, L., Chen, H., Zhang, Y., Yan, S., Chen, X., Gao, X., 2023. Starch granules and their size distribution in wheat: biosynthesis, physicochemical properties and their effect on flour-based food systems. Comput. Struct. Biotechnol. J.

Gupta, R.S., Patel, S., Saini, N., Chen, S., 2020. Robust demarcation of 17 distinct Bacillus species clades, proposed as novel Bacillaceae genera, by phylogenomics and comparative genomic analyses: description of Robertmurraya kyonggiensis sp. nov. and proposal for an emended genus Bacillus limiting it only to the members of the Subtilis and Cereus clades of species. Int. J. Syst. Evolut. Microbiol. 70 (11), 5753–5798.

Haddaway, N.R., Hedlund, K., Jackson, L.E., Kätterer, T., Lugato, E., Thomsen, I.K., Jørgensen, H.B., Isberg, P.-E., 2017. How does tillage intensity affect soil organic carbon? A systematic review. Environ. Evid. 6, 1–48.

Hartig, F., 2022. DHARMa: Residual Diagnostics for Hierarchical (Multi-Level / Mixed) Regression Models. R package version 0.4.6, ⟨https://CRAN.R-project.org/pack age=DHARMa⟩ .

Hartman, K., van der Heijden, Wittwer, R.A., Banerjee, S., Walser, J.-C., Schlaeppi, K., 2018. Cropping practices manipulate abundance patterns of root and soil microbiome members paving the way to smart farming. Microbiome 6, 1–14.

Hartmann, M., Six, J., 2023. Soil structure and microbiome functions in agroecosystems. Nat. Rev. Earth Environ. 4 (1), 4–18.

Helgason, B.L., Walley, F.L., Germida, J.J., 2009. Fungal and bacterial abundance in long-term no-till and intensive-till soils of the Northern Great Plains. Soil Sci. Soc. America J. 73, 120–127.

Hodge, A., Robinson, D., Fitter, A., 2000. Are microorganisms more effective than plants at competing for nitrogen? Trends Plant Sci. 5 (7), 304–308.

Hofmeijer, M.A., Krauss, M., Berner, A., Peigné, J., Mäder, P., Armengot, L., 2019. Effects of reduced tillage on weed pressure, nitrogen availability and winter wheat yields under organic management. Agronomy 9, 180.

Horner-Devine, M.C., Carney, K.M., Bohannan, B.J., 2004, An Ecological Perspective on Bacterial Biodiversity. Proceedings of the Royal Society of London. Series B: Biological Sciences, 271(1535), 113-122..

Hothorn, T., Bretz, F., Westfall, P., 2008. Simultaneous Inference in General Parametric Models. Biom. J. 50 (3), 346–363.

Hu, Y.J., Satten, G.A., 2023. Compositional analysis of microbiome data using the linear decomposition model (LDM). Bioinformatics 39 (11), btad668.

Hutchinson, G.E., 1959. Homage to Santa Rosalia or why are there so many kinds of animals? Am. Nat. 93 (870), 145–159.

Jayasiri, S.C., Hyde, K.D., Jones, E.B.G., McKenzie, E.H.C., Jeewon, R., Phillips, A.J.L., Bhat, D.J., Wanasinghe, D.N., Liu, J.K., Lu, Y.Z., Kang, J.C., Xu, J., Karunarathna, S. C., 2019. Diversity, morphology and molecular phylogeny of Dothideomycetes on decaying wild seed pods and fruits. Mycosphere 10, 1–186.

Jordana, R., Arbea, J.I., 1989. Clave de identificación de los géneros de colémbolos de España (Insecta: Collembola). Publicaciones de Biología de la Universidad de Navarra, Serie Zoológica, 19: 1-16 + 16 lám.

Khianngam, S., Tanasupawat, S., Akaracharanya, A., Kim, K.K., Lee, K.C., Lee, J.S., 2010. Cohnella thailandensis sp. nov., a xylanolytic bacterium from Thai soil. Int. J. Syst. Evolut. Microbiol. 60 (10), 2284–2287.

Kolde, R., 2019. pheatmap: pretty Heatmaps. R. Package Version 1 (0), 12. ⟨http s://CRAN.R-project.org/package=pheatmap⟩.

Krantz, G.W., Walter, D.E., 2009. A Manual of Acarology. 3rd Ed. Texas Tech University Press, Lubbock, p. 807.

Kraut-Cohen, J., Zolti, A., Shaltiel-Harpaz, L., Argaman, E., Rabinovich, R., Green, S.J., Minz, D., 2020. Effects of tillage practices on soil microbiome and agricultural parameters. Sci. Total Environ. 705, 135791.

Kuzyakov, Y., Blagodatskaya, E., 2015. Microbial hotspots and hot moments in soil: Concept & Review. Soil Biol. Biochem. 83, 184–199.

Lenth, R., 2023. emmeans: estimated marginal means, aka least-squares means. R. Package Version 1 (8), 9. ⟨https://CRAN.R-project.org/package=emmeans⟩.

Li, J., Jia, L., Struik, P.C., An, Z., Wang, Z., Xu, Z., Ji, L., Yao, Y., Lv, J., Zhou, T., Jin, K., 2024. Plant and soil responses to tillage practices change arbuscular mycorrhizal fungi populations during crop growth. Front. Microbiol. 15, 1394104.

Li, Y., Li, Z., Cui, S., Jagadamma, S., Zhang, Q., 2019. Residue retention and minimum tillage improve physical environment of the soil in croplands: A global meta-analysis. Soil Tillage Res. 194, 104292.

Lombard, L., Van der Merwe, Groenewald, J.Z., Crous, P.W., 2015. Generic concepts in Nectriaceae. Stud. Mycol. 80 (1), 189–245.

Lori, M., Symnaczik, S., Mäder, P., De Deyn, G., Gattinger, A., 2017. Organic farming enhances soil microbial abundance and activity—A meta-analysis and meta-regression. PloS one 12, e0180442.

Love, M.I., Huber, W., Anders, S., 2014. Moderated estimation of fold change and dispersion for RNA-seq data with DESeq2. Genome Biol. 15 (12), 1–21.

Lücking, R., Lawrey, J.D., Sikaroodi, M., Gillevet, P.M., Chaves, J.L., Sipman, H.J., Bungartz, F., 2009. Do lichens domesticate photobionts like farmers domesticate crops? Evidence from a previously unrecognized lineage of filamentous cyanobacteria. American J. Bot. 96 (8), 1409–1418.

Madigan, M.T., Martinko, J.M., Bender, K.S., Buckley, D.H., 2021. Brock Biology of Microorganisms, 16th Edition. Pearson.

Maechler, M., Rousseeuw, P., Struyf, A., Hubert, M., Hornik, K., 2022. Cluster: Cluster Analysis Basics and Extensions. R. Package Version 2 (1), 4.

Martin, C.A. (2017). ggConvexHull: Add a convex hull geom to ggplot2. R package version 0.1.0, ⟨http://github.com/cmartin/ggConvexHull⟩ .

Martín-Lammerding, D., Hontoria, C., Tenorio, J.L., Walter, I., 2011. Mediterranean dryland farming: effect of tillage practices on selected soil properties. Agron. J. 103 (2), 382–389.

Martín-Lammerding, D., Navas, M., del Mar Albarrán, M., Tenorio, J.L., Walter, I., 2015. Long term management systems under semiarid conditions: influence on labile organic matter, β-glucosidase activity and microbial efficiency. Appl. Soil Ecol. 96, 296–305.

Martín-Lammerding, D., Tenorio, J.L., Albarrán, M.M., Zambrana, E., Walter, I., 2013. Influence of tillage practices on soil biologically active organic matter content over a growing season under semiarid Mediterranean climate. Span. J. Agric. Res. 11 (1), 232–243.

Martin-Rueda, I., Munoz-Guerra, L.M., Yunta, F., Esteban, E., Tenorio, J.L., Lucena, J.J., 2007. Tillage and crop rotation effects on barley yield and soil nutrients on a Calciortidic Haploxeralf. Soil Tillage Res. 92 (1-2), 1–9.

Mathew, R.P., Feng, Y., Githinji, L., Ankumah, R., Balkcom, K.S., 2012. Impact of no-tillage and conventional tillage systems on soil microbial communities. Appl. Environ. Soil Sci. 2012.

Mazor, G., Kidron, G.J., Vonshak, A., Abeliovich, A., 1996. The role of cyanobacterial exopolysaccharides in structuring desert microbial crusts. FEMS Microbiol. Ecol. 21 (2), 121–130.

McCully, M.E., 1999. Roots in soil: unearthing the complexities of roots and their rhizospheres. Annu. Rev. Plant Biol. 50 (1), 695–718.

Mondal, S., Chakraborty, D., 2022. Soil nitrogen status can be improved through no-tillage adoption particularly in the surface soil layer: A global meta-analysis. J. Clean. Prod. 366, 132874.

Morugán-Coronado, A., Pérez-Rodríguez, P., Insolia, E., Soto-Gómez, D., Fernández-Calvino, D., Zornoza, R., 2022. The impact of crop diversification, tillage and fertilization type on soil total microbial, fungal and bacterial abundance: A worldwide meta-analysis of agricultural sites. Agric. Ecosyst. Environ. 329, 107867.

Moyne, O., Al-Bassam, M., Lieng, C., Thiruppathy, D., Norton, G.J., Kumar, M., Haddad, E., Zaramela, L.S., Zengler, K., 2023. Guild and Niche Determination Enable Targeted Alteration of the Microbiome. bioRxiv. Available under: ⟨https://www. ncbi.nlm.nih.gov/pmc/articles/PMC10197622/⟩.

Muñoz-Romero, V., Benítez-Vega, J., López-Bellido, L., López-Bellido, R.J., 2010. Monitoring wheat root development in a rainfed vertisol: tillage effect. Eur. J. Agron. 33 (3), 182–187.

Murugan, R., Koch, H.J., Joergensen, R.G., 2014. Long-term influence of different tillage intensities on soil microbial biomass, residues and community structure at different depths. Biol. Fertil. Soils 50, 487–498.

Nakasaki, K., Saito, M., Suzuki, N., 2007. Coprinellus curtus (Hitoyo-take) prevents diseases of vegetables caused by pathogenic fungi. FEMS Microbiol. Lett. 275 (2), 286–291.

Nguyen, C., 2009. Rhizodeposition of organic C by plant: mechanisms and controls. Sustain. Agric. 97–123.

Nicolas, Y., Martinant, J.P., Denery-Papini, S., Popineau, Y., 1998. Analysis of wheat storage proteins by exhaustive sequential extraction followed by RP-HPLC and nitrogen determination. J. Sci. Food Agric. 77, 96–102.

Nilsson, R.H., Larsson, K.H., Taylor, A.F.S., Bengtsson-Palme, J., Jeppesen, T.S., Schigel, D., Kennedy, P., Picard, K., Glöckner, F.O., Tedersoo, L., Saar, I., 2019. The UNITE database for molecular identification of fungi: handling dark taxa and parallel taxonomic classifications. Nucleic Acids Res. 47 (D1), D259–D264.

Nunes, M.R., Karlen, D.L., Moorman, T.B., 2020. Tillage intensity effects on soil structure indicators—A US meta-analysis. Sustainability 12 (5), 2071.

Oksanen, J., Blanchet, F.G., Kindt, R., Legendre, P., Minchin, P.R., O'hara, R.B., Solymos, P., Stevens, M.H.H., Szoecs, E., Wagner, H., Barbour, M., Bedward, M., Bolker, B., Borcard, D., Carvalho, G., Chirico, M., de Caceres, M., Durand, S., Evangelista, H.B. A., FitzJohn, R., Friendly, M., Furneaux, B., Hannigan, G., O. Hill, M., Lahti, L., McGlinn, D., Ouelette, M.-H., Cunha, E.R., Smith, T., Stier, A., Ter Braak, C.J.F., Weedon, J, 2022. Package 'vegan'. Community ecology package, version, 2.6-4.

Orrù, L., Canfora, L., Trinchera, A., Migliore, M., Pennelli, B., Marcucci, A., Farina, R., Pinzari, F., 2021. How tillage and crop rotation change the distribution pattern of fungi. Front. Microbiol. 12, 634325.

Philippot, L., Chenu, C., Kappler, A., Rillig, M.C., Fierer, N., 2024. The interplay between microbial communities and soil properties. Nat. Rev. Microbiol. 22 (4), 226–239.

Phookamsak, R., Liu, J.K., McKenzie, E.H., Manamgoda, D.S., Ariyawansa, H., Thambugala, K.M., Dai, D.Q., Camporesi, E., Chukeatirote, E., Wijayawardene, N.N.,

Bahkali, A.H., Mortimer, P.E., Xu, J.C., Hyde, K.D., 2014. Revision of Phaeosphaeriaceae. Fungal Divers. 68 (1), 159–238.

Piazza, G., Ercoli, L., Nuti, M., Pellegrino, E., 2019. Interaction between conservation tillage and nitrogen fertilization shapes prokaryotic and fungal diversity at different soil depths: evidence from a 23-year field experiment in the Mediterranean area. Front. Microbiol. 10, 2047.

Pittelkow, C.M., Linquist, B.A., Lundy, M.E., Liang, X., Van Groenigen, K.J., Lee, J., Van Kessel, C., 2015. When does no-till yield more? A global meta-analysis. Field Crops Res. 183, 156–168.

Postma-Blaauw, M.B., de Goede, R.G.M., Bloem, J., Faber, J.H., Brussaard, L., 2010. Soil biota community structure and abundance under agricultural intensification and extensification. Ecology 91 (2), 460–473.

Powell, J.T., Chatziefthimiou, A.D., Banack, S.A., Cox, P.A., Metcalf, J.S., 2015. Desert crust microorganisms, their environment, and human health. J. Arid Environ. 112, 127–133.

Puissant, J., Villenave, C., Chauvin, C., Plassard, C., Blanchart, E., Trap, J., 2021. Quantification of the global impact of agricultural practices on soil nematodes: a meta-analysis. Soil Biol. Biochem. 161, 108383.

Quaedvlieg, W., Kema, G.H.J., Groenewald, J.Z., Verkley, G.J.M., Seifbarghi, S., Razavi, M., Mirzadi Gohari, A., Mehrabi, R., Crous, P.W., 2011. Zymoseptoria gen. nov.: a new genus to accommodate Septoria-like species occurring on graminicolous hosts. Pers.-Mol. Phylogeny Evol. Fungi 26 (1), 57–69.

Quast, C., Pruesse, E., Yilmaz, P., Gerken, J., Schweer, T., Yarza, P., Peplies, J., Glöckner, F.O., 2012. The SILVA ribosomal RNA gene database project: improved data processing and web-based tools. Nucleic Acids Res. 41 (D1), D590–D596.

R Core Team, 2023. R: A Language and Environment for Statistical Computing. R Foundation for Statistical Computing, Vienna, Austria. ⟨https://www.R-project.org/⟩ .

Ramírez, P.B., Fuentes-Alburquenque, S., Díez, B., Vargas, I., Bonilla, C.A., 2020. Soil microbial community responses to labile organic carbon fractions in relation to soil type and land use along a climate gradient. Soil Biol. Biochem. 141, 107692.

Roger-Estrade, J., Anger, C., Bertrand, M., Richard, G., 2010. Tillage and soil ecology: partners for sustainable agriculture. Soil Tillage Res. 111 (1), 33–40.

Rousseeuw, P.J., 1987. Silhouettes: a graphical aid to the interpretation and validation of cluster analysis. J. Comput. Appl. Math. 20, 53–65.

Salgado-Salazar, C., Beirn, L.A., Ismaiel, A., Boehm, M.J., Carbone, I., Putman, A.I., Tredway, L.P., Clarke, B.B., Crouch, J.A., 2018. Clarireedia: A new fungal genus comprising four pathogenic species responsible for dollar spot disease of turfgrass. Fungal Biol. 122 (8), 761–773.

Santín-Montanyá, M.I., Casanova Pena, C., Zambrana Quesada, E., Sánchez Jiménez, F. J., Tenorio Pasamón, J.L., 2018. Arable weed species associated with soil tillage systems under Mediterranean conditions. Land Degrad. Dev. 29 (4), 865–874.

Santín-Montanyá, M.I., Fernández-Getino, A.P., Zambrana, E., Tenorio, J.L., 2017. Effects of tillage on winter wheat production in Mediterranean dryland fields. Arid Land Res. Manag. 31 (3), 269–282.

Santín-Montanyá, M.I., Gandía-Toledano, M.L., Zambrana, E., Tenorio, J.L., 2020. Effects of tillage systems on wheat and weed water relationships over time when growing together, in semiarid conditions. Ann. Appl. Biol. 177 (2), 256–265.

Santín-Montanyá, M.I., Martín-Lammerding, D., Walter, I., Zambrana, E., Tenorio, J.L., 2013. Effects of tillage, crop systems and fertilization on weed abundance and diversity in 4-year dry land winter wheat. Eur. J. Agron. 48, 43–49.

Santín-Montanyá, M.I., Martín-Lammerding, D., Zambrana, E., Tenorio, J.L., 2016. Management of weed emergence and weed seed bank in response to different tillage, cropping systems and selected soil properties. Soil Tillage Res. 161, 38–46.

Scherer, H.W., Weichmann, H., 1994. Die Bestimmung des pflanzenverfügbaren Phosphors und Kaliums in Böden mit der CAL-Methode. J. Plant Nutr. Soil Sci. 157 (3), 227–232. https://doi.org/10.1002/jpln.19941570311).

Schloss, P.D., 2024. Rarefaction is currently the best approach to control for uneven sequencing effort in amplicon sequence analyses. Msphere, e00354-23.

Seethepalli, A., Dhakal, K., Griffiths, M., Guo, H., Freschet, G.T., York, L.M., 2021. RhizoVision Explorer: open-source software for root image analysis and measurement standardization. AoB Plants 13 (6), plab056.

Shewry, P.R., Van Schaik, F., Ravel, C., Charmet, G., Rakszegi, M., Bedo, Z., Ward, J.L., 2011. Genotype and environment effects on the contents of vitamins B1, B2, B3, and B6 in wheat grain. J. Agric. Food Chem. 59 (19), 10564–10571.

Six, J., Frey, S.D., Thiet, R.K., Batten, K.M., 2006. Bacterial and fungal contributions to carbon sequestration in agroecosystems. Soil Sci. Soc. Am. J. 70 (2), 555–569.

Slowikowski, K., 2023. ggrepel: Automatically Position Non-Overlapping Text Labels with 'ggplot2'. R package version 0.9.4, ⟨https://CRAN.R-project.org/package=ggrepel⟩ .

Strunecký, O., Ivanova, A.P., Mareš, J., 2023. An updated classification of cyanobacterial orders and families based on phylogenomic and polyphasic analysis. J. Phycol. 59 (1), 12–51.

Symanczik, S., Krauss, M., Bodenhausen, N., Declerck, S., Doubell, M., Faist, H., Kundel, D., 2025. Performance of different wheat varieties and their associated microbiome under contrasting tillage and fertilization intensities: Insights from a Swiss long-term field experiment. Soil Tillage Res. 246, 106328.

Tedersoo, L., Lindahl, B., 2016. Fungal identification biases in microbiome projects. Environ. Microbiol. Rep. 8 (5), 774–779.

Tellez-Rio, A., Vallejo, A., Garcia-Marco, S., Martin-Lammerding, D., Tenorio, J.L., Rees, R.M., Guardia, G., 2017. Conservation agriculture practices reduce the global warming potential of rainfed low N input semi-arid agriculture. Eur. J. Agron. 84, 95–104.

Tibshirani, R., Walther, G., Hastie, T., 2001. Estimating the number of clusters in a data set via the gap statistic. J. R. Stat. Soc. Ser. B (Stat. Methodol. 63 (2), 411–423.

Trachsel, S., Kaeppler, S.M., Brown, K.M., Lynch, J.P., 2011. Shovelomics: high throughput phenotyping of maize (Zea mays L.) root architecture in the field. Plant Soil 341 (1–2), 75–87. https://doi.org/10.1007/s11104-010-0623-8.

van Capelle, C., Schrader, S., Brunotte, J., 2012. Tillage-induced changes in the functional diversity of soil biota–A review with a focus on German data. Eur. J. Soil Biol. 50, 165–181.

Van Groenigen, Bloem, J., Bååth, E., Boeckx, P., Rousk, J., Bodé, S., Jones, M.B., 2010. Abundance, production and stabilization of microbial biomass under conventional and reduced tillage. Soil Biol. Biochem. 42 (1), 48–55.

VDLUFA, 1991. Bestimmung von Schwermetallen im Aufschluss mit Königswasser. Verband Deutscher Landwirtschaftlicher Untersuchungs- und Forschungsanstalten (VDLUFA) Methodenbuch Band I, A 2.4.3.1. VDLUFA-Verlag, Darmstadt, Germany, pp. 1-5..

VDLUFA, 2008. Bestimmung von Haupt- und Spurennährstoffen in Kultursubstraten im Calciumchlorid/DTPA-Auszug (CAT-Methode). Herstellung des Extraktes. Verband Deutscher Landwirtschaftlicher Untersuchungs- und Forschungsanstalten (VDLUFA) Methodenbuch Band II.2, 1. Ergänzung., Stickstoff, CaCl2-DTPA-Auszug 3.7.1.2, VDLUFA-Verlag, Darmstadt, Germany, pp. 1-6.

VDLUFA, 2012. Bestimmung von Gesamt-Stickstoff nach trockener Verbrennung (Elementaranalyse). Verband Deutscher Landwirtschaftlicher Untersuchungs- und Forschungsanstalten (VDLUFA) Methodenbuch Band I, 6. Teillieferung, A 2.2.5, VDLUFA-Verlag, Darmstadt, Germany, pp. 1-6.

VDLUFA, 2016. Bestimmung von Phosphor und Kalium im Calcium-Acetat-Lactat-Auszug. Verband Deutscher Landwirtschaftlicher Untersuchungs- und Forschungsanstalten (VDLUFA). Methodenbuch Band I: Die Untersuchung von Böden, 7. Teillieferung. A 6.2.1.1. VDLUFA-Verlag, Darmstadt, Germany, pp. 1-8.

VDLUFA, 2019. Ionenchromatographische Bestimmung. Verband Deutscher Landwirtschaftlicher Untersuchungs- und Forschungsanstalten (VDLUFA), Methodenbuch Band II.2 3. Ergänzung 2.2-4.7.2.2, VDLUFA-Verlag, Darmstadt, Germany, pp. 1-4.

VDLUFA, 2021. Mikrowellenbeheizter Druckaufschluß 2021-03. Verband Deutscher Landwirtschaftlicher Untersuchungs- und Forschungsanstalten (VDLUFA) Methodenbuch Band VII, Umweltanalytik, 2.1.3. VDLUFA-Verlag, Darmstadt, Germany, pp. 1-5.

Wagg, C., Hautier, Y., Pellkofer, S., Banerjee, S., Schmid, B., van der Heijden, M.G., 2021. Diversity and asynchrony in soil microbial communities stabilizes ecosystem functioning. elife 10, e62813.

Wagg, C., Schlaeppi, K., Banerjee, S., Kuramae, E.E., van der Heijden, M.G., 2019. Fungal-bacterial diversity and microbiome complexity predict ecosystem functioning. Nat. Commun. 10 (1), 4841.

Wang, H., Wang, S., Wang, R., Wang, X., Li, J., 2020. Conservation tillage increased soil bacterial diversity and improved soil nutrient status on the Loess Plateau in China. Arch. Agron. Soil Sci. 66, 1509–1519.

Wardle, D.A., Ghani, A.A., 1995. A critique of the microbial metabolic quotient (qCO2) as a bioindicator of disturbance and ecosystem development. Soil Biol. Biochem. 27 (12), 1601–1610.

Watt, M., Kirkegaard, J.A., Rebetzke, G.J., 2005. A wheat genotype developed for rapid leaf growth copes well with the physical and biological constraints of unploughed soil. Funct. Plant Biol. 32 (8), 695–706.

Watt, M., Magee, L.J., McCully, M.E., 2008. Types, structure and potential for axial water flow in the deepest roots of field-grown cereals. N. Phytol. 178 (1), 135–146.

Watt, M., Schneebeli, K., Dong, P., Wilson, I.W., 2009. The shoot and root growth of Brachypodium and its potential as a model for wheat and other cereal crops. Funct. Plant Biol. 36 (11), 960–969.

Wickham, H., Averick, M., Bryan, J., Chang, W., McGowan, L.D., François, R., Grolemund, G., Hayes, A., Henry, L., Hester, J., Kuhn, M., Pedersen, T.L., Miller, E., Bache, S.M., Müller, K., Ooms, J., Robinson, D., Seidel, D.P., Spinu, V., Takahashi, K., Vaughan, D., Wilke, C., Woo, K., Yutani, H., 2019. Welcome to the tidyverse. J. Open Source Softw. 4 (43), 1686. https://doi.org/10.21105/joss.01686. ⟨https://doi.org/10.21105/joss.01686⟩.

Wieser, H., Antes, S., Seilmeier, W., 1998. Quantitative determination of gluten protein types in wheat flour by reversed-phase high-performance liquid chromatography. Cereal Chem. 75, 644–650.

Yang, L., Chen, J., 2022. A comprehensive evaluation of microbial differential abundance analysis methods: current status and potential solutions. Microbiome 10 (1), 130.

Yang, L., Chen, J., 2023. Benchmarking differential abundance analysis methods for correlated microbiome sequencing data. Brief. Bioinf. 24 (1), bbac607.

Yeates, G.W., 1994. Modification and Qualification of the Nematode Maturity index.

Young, M.D., Ros, G.H., de Vries, W., 2021. Impacts of agronomic measures on crop, soil, and environmental indicators: A review and synthesis of meta-analysis. Agric. Ecosyst. Environ. 319, 107551.

Zeileis, A., Hothorn, T., 2002. Diagnostic checking in regression relationships. R. N. 2 (3), 7–10. ⟨https://CRAN.R-project.org/doc/Rnews/⟩.

Zhang, H., Song, G., Shao, J., Xiang, X., Li, Q., Chen, Y., Yang, P., Yu, G., 2016. Dynamics and polyphasic characterization of odor-producing cyanobacterium Tychonema bourrellyi from Lake Erhai, China. Environ. Sci. Pollut. Res. 23, 5420–5430.

Zhou, H., He, K., Chen, J., Zhang, X., 2022. LinDA: linear models for differential abundance analysis of microbiome compositional data. Genome Biol. 23 (1), 1–23.